



Universidade do Minho  
Escola de Engenharia

Luís Miguel Rios Vieira  
Continuous evaluation of the stiffness of stabilized soils since  
compaction: enhancements to the EMM-ARM methodology

Luís Miguel Rios Vieira

Continuous evaluation of the stiffness of  
stabilized soils since compaction:  
enhancements to the EMM-ARM methodology





Universidade do Minho  
Escola de Engenharia

Luís Miguel Rios Vieira

Continuous evaluation of the stiffness of  
stabilized soils since compaction:  
enhancements to the EMM-ARM methodology

Master's Thesis  
Integrated Ms Civil Engineering

Work performed under the supervision of  
Professor António Gomes Correia

And co-supervision of  
Professor Miguel Azenha

## DECLARAÇÃO

Luís Miguel Rios Vieira

Endereço electrónico: luisriosrios@hotmail.com

Telefone:963489208

Número do Bilhete de Identidade: 13781254

Título dissertação

Continuous evaluation of the stiffness of stabilized soils since compaction enhancements to the EMM-ARM methodology

Orientador:

Professor António Gomes Correia

Professor Miguel Azenha

Ano de conclusão: 2014

Designação do Mestrado

Ciclo de Estudos Integrados Conducentes ao Grau de Mestre em Engenharia Civil

Nos exemplares das teses de doutoramento ou de mestrado ou de outros trabalhos entregues para prestação de provas públicas nas universidades ou outros estabelecimentos de ensino, e dos quais é obrigatoriamente enviado um exemplar para depósito legal na Biblioteca Nacional e, pelo menos outro para a biblioteca da universidade respectiva, deve constar uma das seguintes declarações:

É AUTORIZADA A REPRODUÇÃO INTEGRAL DESTA TESE APENAS PARA EFEITOS DE INVESTIGAÇÃO, MEDIANTE DECLARAÇÃO ESCRITA DO INTERESSADO, QUE A TAL SE COMPROMETE.

Universidade do Minho, \_\_\_/\_\_\_/\_\_\_\_\_

Assinatura: \_\_\_\_\_

## **Acknowledgments**

I would like to thank to all persons who made this dissertation possible namely:

- Professor António Gomes Correia, supervisor of this dissertation, for his advices and for sharing his knowledge and experience.
- Professor Miguel Azenha, co-supervisor of this dissertation, for his enthusiasm, motivation and help especially in the writing process;
- PhD student Jacinto Silva for his patient, motivation and availability throughout this entire work;
- all technicians in the Civil Engineering Laboratory at University of Minho for their help during the experimental programs particularly to Mr. José Gonçalves;
- my parents for their incredible support throughout my academic course.



## **Abstract**

The stabilization of soils has been used for the improvement of its characteristics to meet required performances. Binders are widely used for the stabilization process, and thereby the soil suffers a hardening process during which its mechanical properties are improved, namely its stiffness. Monitoring the stiffness evolution over the hardening time can reveal important information for quality control, and early identification of potential problems. The EMM-ARM (Elasticity Modulus Measurement through Ambient Response Method) has been applied to stabilized soils in pursuit of a robust method that actually allows continuous measurement of the stiffness of a stabilized soil since very early ages. EMM-ARM is based on the identification of the resonance frequency of a composite beam that comprises the tested material, over the curing time and allows inferring the E-modulus of the stabilized time through the dynamic equation of motion of the beam.

This technique has been used on stabilized soils with success. However, the technique still lacked a sampling method that allowed retrieving representative samples from in-situ layers. This dissertation aimed to contribute for the development of the EMM-ARM technique namely in developing a sampling procedure that can be applied on practical conditions. Therefore, a specific sampler was developed for EMM-ARM, and its feasibility has been proved through an experimental program for validation.

Moreover a new EMM-ARM variant that allows direct in-situ tests was proposed in order to avoid the uncertainties related with the sampling process. This variant consists on the identification of the resonance frequency of a steel bar that is partially embedded in the tested layer of stabilized soil. Even though the pilot applications revealed sensitive issues of the proposed technique, its viability and feasibility has potential to be further improved.

### **Key Words**

Stabilization, Cement, E-modulus, Sampling, EMM-ARM





## Resumo

A estabilização de solos tem sido usada para o melhoramento das suas características para o cumprimento de requisitos de desempenho. Os ligantes são amplamente utilizados para o processo de estabilização, e desse modo o solo sofre um processo de endurecimento durante o qual as suas propriedades mecânicas são melhoradas nomeadamente a sua rigidez. A monitorização da evolução da rigidez ao longo do período de endurecimento pode revelar informações importantes para o controlo da qualidade e para a identificação de potenciais problemas. A técnica EMM-ARM (Elasticity Modulus Measurement through Ambient Response Method) tem sido aplicado a solos estabilizados de forma a encontrar um método que realmente permita a medição contínua da rigidez de solos estabilizados desde as primeiras idades. O EMM-ARM é baseado na identificação da frequência de ressonância de uma viga mista que inclui o material a testar, ao longo do período de cura e permite deduzir o módulo de elasticidade no tempo de estabilização através de equações de equilíbrio dinâmico.

Esta técnica tem sido usada com sucesso em solos estabilizados. Contudo a técnica ainda não possui um método de amostragem que permita a recolha de amostras representativas de camadas estabilizadas in-situ. Esta dissertação tem o propósito de contribuir para o desenvolvimento da técnica EMM-ARM nomeadamente em desenvolver um processo de amostragem que possa ser aplicado em condições reais de campo. Neste contexto, foi desenvolvido um amostrador específico para o EMM-ARM, e a sua viabilidade foi comprovada através da execução de um programa experimental.

Além disso foi proposto uma nova variante do EMM-ARM que permite ensaios in-situ de forma a evitar as incertezas relacionadas com a amostragem. Esta nova modalidade de ensaio consiste em identificar a frequência de ressonância de uma viga de aço parcialmente embebida numa camada de solo estabilizado. Apesar da aplicação piloto ter revelado alguns problemas de sensibilidade da técnica proposta, a sua potencialidade merece aperfeiçoamento futuro.

Palavras-chave

Estabilização, Cimento, Deformabilidade, Amostragem, EMM-ARM



## Table of Contents

1	INTRODUCTION .....	1
1.1	General remarks .....	1
1.2	Dissertation Structure .....	3
2	EXPERIMENTAL ASSESSMENT OF THE ELASTICITY MODULUS IN STABILIZED SOILS .....	4
2.1	Laboratory tests.....	4
2.1.1	EMM-ARM .....	4
2.1.2	Uniaxial compression test.....	11
2.1.3	Bender elements .....	12
2.1.4	Ultrasonic tests .....	13
2.2	Field tests .....	15
2.2.1	Static load plate test.....	15
2.2.2	Light Weight Deflectometer .....	16
2.2.3	Humbolt stiffness gauge .....	17
2.3	E-modulus vs strain level.....	18
2.4	Overall summary table.....	20
3	DEVELOPMENT OF SAMPLER .....	21
3.1	Sampling: general considerations .....	21
3.2	Block sampling .....	21
3.3	Tube Samplers .....	23
3.3.1	Design considerations.....	23
3.3.2	Drive samplers.....	26
3.3.3	Rotary Samplers .....	31
3.4	Sample driving techniques.....	32
3.5	Summary of sampler types .....	35
3.6	Sampling for EMM-ARM: existing procedures .....	36

3.7	Proposed sampler and driving technique .....	38
<b>4</b>	<b>EXPERIMENTAL PROGRAM .....</b>	<b>43</b>
4.1	Materials and mixture proportions.....	43
4.1.1	Soil.....	43
4.1.2	Cement.....	45
4.1.3	Mixture proportions .....	45
4.2	Pilot application .....	46
4.2.1	Overall Strategy .....	46
4.2.2	Preparation of the mixture and placement.....	47
4.2.3	Sampling.....	48
4.2.4	Description of the test procedures for E evaluation .....	49
4.2.5	Results .....	51
<b>5</b>	<b>PROPOSAL OF A VARIANT OF EMM-ARM.....</b>	<b>55</b>
5.1	Concept .....	55
5.2	Proposed pilot model .....	57
5.2.1	Performance requirements .....	57
5.2.2	Preliminary numerical studies .....	58
5.2.3	Detailed simulations of the proposed setup.....	59
5.3	Pilot experiments .....	62
5.3.1	Experimental setup .....	62
5.3.2	Strategy and procedures.....	63
5.3.3	Results .....	66
5.3.4	Evaluation in view of numerical simulations .....	67
<b>6</b>	<b>Conclusion .....</b>	<b>71</b>
6.1	General conclusions .....	71
6.2	Future Developments .....	72
<b>7</b>	<b>Bibliography.....</b>	<b>73</b>

## List of Figures

Figure 1 - Resonant frequency identification process over testing time (Silva <i>et al.</i> 2013) adapted.....	5
Figure 2 - Comparison between compression tests(blue) and EMM-ARM technique (Azenha 2009) .....	6
Figure 3 - U-shaped cross section (Silva 2010).....	7
Figure 4 - Tubular PVC mould: (a) cross-section; (b) lateral view (units: mm) (Silva <i>et al.</i> 2013).....	8
Figure 5 - The windows of Hanning with 50% overlap .....	9
Figure 6 - Average of the FFT segments.....	10
Figure 7 - Sketch of half-beam.....	11
Figure 8 - Uniaxial compression test with LVDTs mounted (Silva 2010).....	12
Figure 9 - Sketch of a Bender elements setup after(Alvarado & Coop 2012).....	13
Figure 10 - Schematic Ultrasonic setup (Yesiller <i>et al.</i> 2001) .....	15
Figure 11 - Load Cell and Plate Set Up from NCDOT .....	16
Figure 12 - Light Weight Deflectometer (Adam & Adam 2003).....	17
Figure 13 - Humbolt equipment .....	18
Figure 14 - Steps of the Simpson model compared with the real stiffness-strain curve (Benz 2007).....	19
Figure 15 - Moduli as a function of strain level for various numerical simulations and test analysis .....	19
Figure 16 - Schematic diagram of the Sherbrooke down-hole block sampler (Lefebvre & Poulin 1979) .....	22
Figure 17 - Dimensions of a tube sampler (Clayton <i>et al.</i> 1998) .....	23
Figure 18 - Influence of AR in sample quality (Siddique <i>et al.</i> 2006) .....	24
Figure 19 - Analytical solutions for axial strain history at the center-line of the sampler for different B/t ratio (Clayton <i>et al.</i> 1998).....	25
Figure 20 - Shelby tube available at the University of Minho .....	27
Figure 21 - Scheme of theU100 sampler (Bell 2004).....	28
Figure 22 - SPT Sampler .....	28
Figure 23 - Sampler with stationary piston (Nagaraj 1993) .....	30

Figure 24 - Osterberg hydraulic piston sampler (Osterberg 1973).....	31
Figure 25 - a) Single tube corebarrel (Murthy 2002) b) Denison triple-tube corebarrel (Johnson 1940) .....	32
Figure 26 - X-ray photographs of sampling by hammering (left) and pushed (right) (Briaud 2013).....	34
Figure 27 - Slide hammer (Hmtri 1997).....	34
Figure 28 - Prismatic mould: a) Lateral view; b) cross-section; c) scheme of the set sampler / mould (Silva <i>et al.</i> 2014).....	36
Figure 29 - Phases of the sampling process with the prismatic mould (Silva <i>et al.</i> 2014)..	37
Figure 30 - Details of the sampling with the PVC tube (Costa 2011).....	38
Figure 31 - Dimensions of the sampler (mm).....	39
Figure 32 - Sampler and detail of the cutting edge.....	40
Figure 33 - Preliminary test.....	41
Figure 34 - Driving procedure.....	42
Figure 35 - Granulometric curve of the sand.....	44
Figure 36 - Compaction curve of the Sand.....	45
Figure 37 - Compaction curve of the Sand-Cement mixture.....	46
Figure 38 - Overall Strategy .....	47
Figure 39 - Preparation of the UCC Specimen adapted from (Magalhães 2013).....	48
Figure 40 - Apparatus of the sampling .....	49
Figure 41 - EMM-ARM test.....	50
Figure 42 - a) accelerometer b) signal acquisition system (Costa 2011).....	50
Figure 43 - UCC setup.....	51
Figure 44 - Load-Displacement curve for the sampler.....	52
Figure 45 - EMM-ARM results.....	53
Figure 46 - UCC stress-strain relationship .....	53
Figure 47 - EMM-ARM vs UCC test results.....	54
Figure 48 - Scheme of the concept .....	56
Figure 49 - Schematic showing transducer and specimen well connected to charge amplifier, frequency response analyser and personal computer (Meredith 1999) .....	57
Figure 50 - Sketch of the proposed model (dimensions in mm) and 3d view from Multiphysics .....	59
Figure 51 - Numerical model.....	60

Figure 52 - Computed relationship between the resonant frequency of the embedded steel bar and the E-modulus of the tested material .....	61
Figure 53 - Derivative of the frequency .....	61
Figure 54 - Beam used and sharpened edge .....	63
Figure 55 - PVC container.....	63
Figure 56 - a) PVC tube with the wooden pestle b) Plastic sheet involving the container .	64
Figure 57 - Scheme of the guide (dimension in mm) .....	65
Figure 58 - Beam with the guide .....	65
Figure 59 - Setup in a preliminary test .....	66
Figure 60 - Results in frequency domain .....	66
Figure 61 - Results of the new technique compared with the results of the previous chapter .....	67
Figure 62 - Results of B1 with an elasticity modulus of 205 GPa and 210 GPa.....	68
Figure 63 - Results of the bar 2 for a 15,3-15,4cm length of the cantilever.....	69
Figure 64 - Results of the bar 3 for a 15,3-15,4cm length of the cantilever.....	69

## List of Tables

Table 1 - Assessment tests summary .....	20
Table 2 - Combinations of AR and OCE.....	26
Table 3 - Hvorslev's driving methods as in (Nagaraj 1993).....	33
Table 4 - Summary of the samplers.....	35
Table 5 - Grain size of the sand.....	43
Table 6 - UCC specimens results .....	54
Table 7 - The three first modes.....	62

## Glossary

EMM-ARM	(Elasticity Modulus Measurement through Ambient Response Method)
AR	Ratio of area
BE	Bender Element
$\varepsilon$	Strain

E	Elasticity Modulus
$E_{LFW D}$	Strain Modulus
$E_{v2}$	Strain Modulus
$E_{SSG}$	Soil Strain Modulus
FFT	Fast Fourier Transform
G	Shear Modulus
$H_1$	Internal height along the cutting edge
$H_2$	External height along the cutting edge
I	Inertia
ICA	Inside cutting angle
ICR	Inside clearance ratio
ltt	Distance tip-to-tip
LVDT	Linear Variable Differential Transformer
LWD	Light Weight Deflectometer
M	Constrained Modulus
OCA	Outside cutting angle
OCE	Overall cutting edge
PVC	Polyvinyl chloride
R	External Radius
$R_1$	Radius at the bottom edge of the sampler
$R_2$	Radius along the sampler
t	Tickness
tt	Travel Time
UCC	Unconfined compression cyclic tests
VEM-STIFF	Very Early age Material Stiffness Monitoring
$V_p$	P Wave Velocity
$V_s$	Shear Wave Velocity
$\nu$	Poisson's ratio
w	First Flexural Resonance Frequency
$\alpha$	External cutting angle
$\beta$	Internal cutting angle



# 1 INTRODUCTION

## 1.1 General remarks

The behavior of a foundation soil is decisive for the performance of civil engineering structures. Frequently soil characteristics fail to meet the necessary performance requirements to ensure structural safety. In such cases, the soil may be replaced by a better performing material. However, this can be quite impractical and expensive. Therefore, a frequently adopted alternative consists in improving the existing soil properties through a process that is known as stabilization. The stabilization of soils may be achieved by its mechanical compaction or through the addition of chemical additives such as cement or lime. Soil stabilization may improve several properties, such as the soil swelling potential, permeability, shearing and compressive strength (Anifowose 1989; Bell 1993). The use of cement or lime to improve the geotechnical characteristics of soils has become widely used because it allows customized control of the properties of the material through the proportions of the mixture, while being quite feasible from the economic point of view (Horpibulsuk *et al.* 2006; Quigley 2006).

According to Quigley (2006) the traditional stabilization process through chemical additions includes four main stages:

- lime or cement uniformly spread by mechanical means;
- mixing and pulverization of the soil;
- trim and lightly compact followed by mellowing for a period of time;
- heavy compaction to ensure air voids of 5% or less.

The geotechnical behavior of treated soils depends on its chemical and physical properties, that are directly related with the soil formation conditions and mineralogical composition (Kennedy *et al.* 1987).

Lime stabilization is more suitable for soils with high content of clay while cement can be used in any soil with the exception of highly organic soils or some highly plastic clays (Bell 1993; Amu *et al.* 2011).

As concluded by Nagaraj *et al.* (2014) the combination of cement and lime can be mutual beneficial in some cases as in earth blocks because cement stabilizes the sand portion of the soil whereas lime stabilizes the clay portion.

The chemical stabilization techniques have been used in pavements base layers, slope protection, channel linings, to prevent liquefaction and as a base layer to shallow foundations ( Bell 1993; Consoli *et al.* 2011; Portelinha *et al.* 2012).

The ratio binder-soil needs to be determined in laboratory tests in order to control the performance of the mixture in achieving the target proprieties in terms of stiffness, strength and durability. This experimentally based determination of mix proportions is necessary because there are no general methodologies established on rational criteria for the prediction of the mechanical proprieties based on the mixture (Viana da Fonseca *et al.* 2009).

According to Consoli *et al.* (2011), dosage methodologies and soil-cement strength have been most conveniently assessed by unconfined compression tests. This technique allows the assessment of the small-strain stiffness of the tested material. However its use at early ages is limited due to the lack of strength of the material that induces relevant experimental difficulties in handling and loading.

Other techniques have been used for the measurement of the small-strain stiffness namely techniques based on wave propagation such as the bender elements (Ferreira 2009) or the ultrasonic tests (Yesiller *et al.* 2001). These techniques allow non-destructive tests without affecting the properties of the material although these techniques have some uncertainties on the interpretation of results.

A new technique called EMM-ARM has been proposed in 2009 (Azenha 2009) to continuously and automatically measure the stiffness of concrete and cement paste since the fresh state (i.e. right after casting). More recent research works have shown the feasibility of application of EMM-ARM on testing the stiffness of stabilized soils (Silva 2010). This methodology allows overcoming the main limitation of the unconfined compression tests of its use at early ages. Moreover it allows the continuous monitoring instead of discrete instants of time. Compared with the benders and ultrasonic the results of the EMM-ARM technique do not have the uncertainties associated with the wave propagation techniques.

Despite the success of EMM-ARM applications to stabilized soils it requires the specimen to be reconstituted in the mould in order to perform the test. However recent applications (Silva *et al.* 2014) included a preliminary sampling process that proved the feasibility of sampling on EMM-ARM but without the required robustness.

This dissertation has the purpose of contributing for the development of the EMM-ARM technique, particularly in concern to the sampling procedure. The dissertation also outlines an initial attempt for a variant to EMM-ARM that allows direct in-situ testing of a stabilized soil without needing to extract samples (VEM-STIFF technique).

## **1.2 Dissertation Structure**

Besides the present introduction, Chapter 2 provides a literature review of methods for assessment of the elasticity modulus with special emphasis to the EMM-ARM technique.

In Chapter 3 a new sampler and sampling technique are proposed for the EMM-ARM methodology. This chapter includes a literature review of existing samplers and previous attempts of EMM-ARM application that included sampling.

Chapter 4 concerns the practical application of the developed sampler, within the scope of a validation experimental program.

A new variant of the EMM-ARM technique is proposed in Chapter 5, where a set of pilot experiments are presented.

The dissertation is closed by an outline of its main conclusions and prospected further developments (Chapter 6).

## **2 EXPERIMENTAL ASSESSMENT OF THE ELASTICITY MODULUS IN STABILIZED SOILS**

### **2.1 Laboratory tests**

#### **2.1.1 EMM-ARM**

##### **2.1.1.1 Concept**

EMM-ARM (Elasticity Modulus Measurement through Ambient Response Method) is a technique that allows the continuous measurement of the elasticity modulus of hardening materials (e.g. cement-based materials) since early ages. In its original implementation (Azenha 2009), this methodology consisted in successively identifying the first flexural resonance frequency of a simply supported composite beam composed by an external mould which is internally filled with the material to test (concrete). The technique assumes that the ambient vibration is sufficient to excite the beam for the output-only modal identification. As can be seen in Figure 1 the identification of the resonance frequency is repeated over the time through the measurement of the accelerations (a), which are converted into the frequency-domain (b). It is then possible to obtain a frequency-time curve of the beam (c).

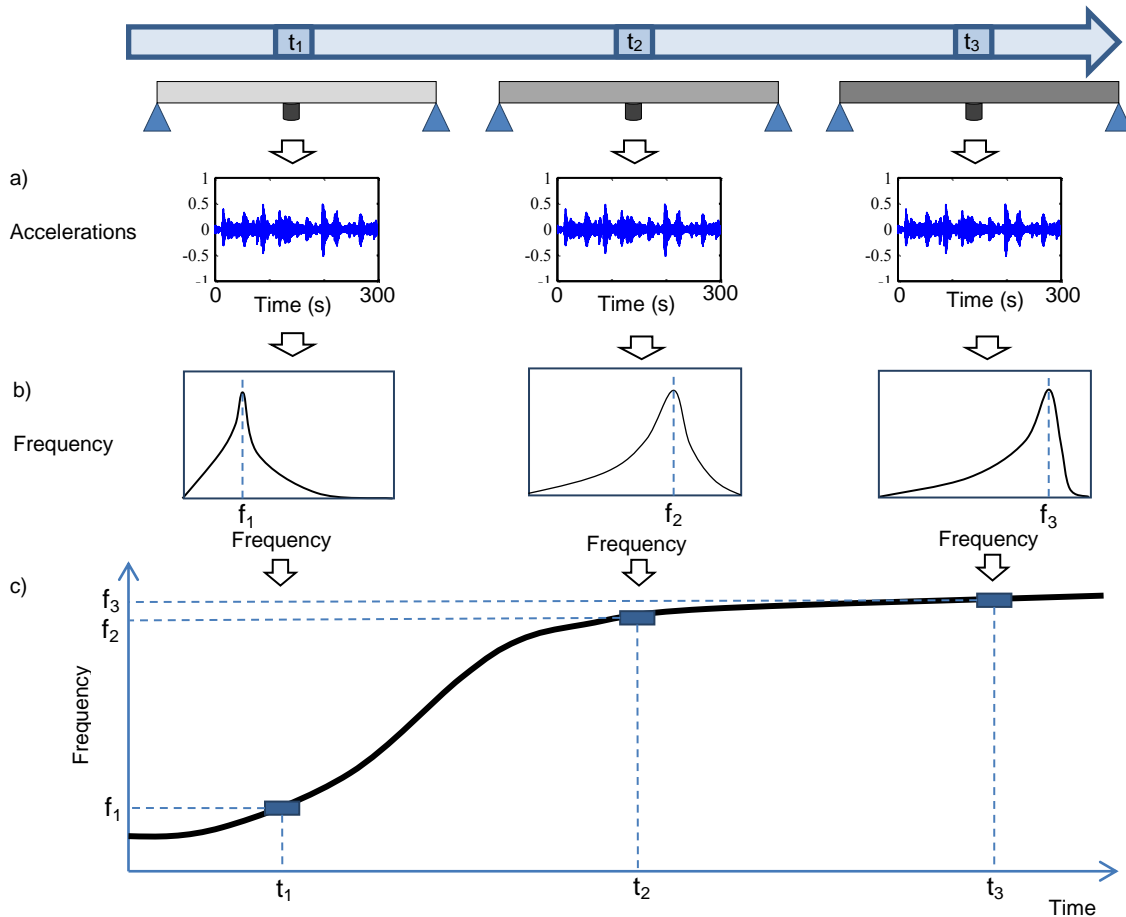


Figure 1 - Resonant frequency identification process over testing time (Silva *et al.* 2013) adapted

The identified resonant frequency is then correlated with the elasticity modulus of the tested material through application of the dynamic equation of motion of the simply supported beam (Silva *et al.* 2013). It is therefore possible to convert the frequency-time curve into the desired elasticity modulus-time curve.

### 2.1.1.2 Developments in EMM-ARM since its creation

The first application of the EMM-ARM technique was performed in concrete (Azenha 2009). The pilot experiment was accomplished through a simply supported 2-meter acrylic tube of 0,1m diameter, filled with concrete, put into simply supported conditions and placed within a controlled temperature and humidity. The material was monitored in the first 28 days with an accelerometer which allowed the identification of the first flexural resonance frequency of the beam in that period. The frequency was then correlated with

the elasticity modulus. To validate the EMM-ARM results, cyclic compressive tests were performed in cylinders for comparative purposes. The Figure 2 shows the results:

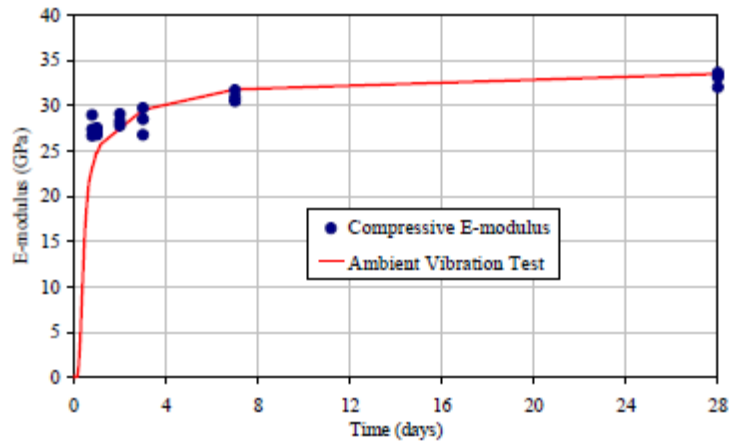


Figure 2 - Comparison between compression tests(blue) and EMM-ARM technique (Azenha 2009)

As can be seen in Figure 2 the compressive tests corroborated the feasibility of EMM-ARM. Following the success of the application in concrete, the technique was then successfully tested in cement pastes (Azenha 2009).

The application of the technique to stabilized soils was then tested by Silva (2010). As the sand-cement materials have a lower elasticity modulus than concrete it was necessary to adapt the technique to these materials thus the mould was redesigned to ensure that the range of resonant frequencies during the experiment was large enough to allow the proper identification of stiffness evolution (Silva *et al.* 2013). The new mould was made of polycarbonate and had a U-shaped cross-section with an inner size of 40mm x 40mm, as shown in Figure 3 and a span of 495mm. This mould also had the interesting particularity of being reusable.

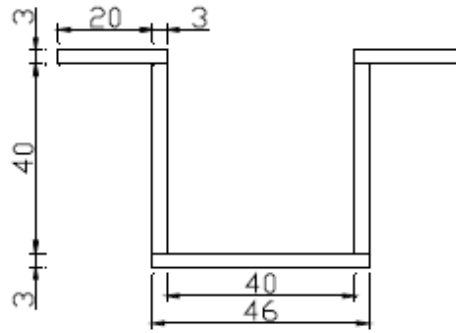


Figure 3 - U-shaped cross section (Silva 2010)

Even though the pilot experiments were considered successful, Silva *et al.* (2013) reported some important drawbacks: (i) due to the low slenderness of the mould, the frequencies are much higher than in previous applications in concrete, making the specimen less excitable and thus making modal identification more difficult; (ii) the material to be tested needs to be compacted directly into the mould which may complicate the replication of in-situ conditions in terms of compaction level.

Silva (2010) has overcome the above-mentioned limitations with a new design for the mould. The new mould is a 50 mm-diameter PVC tube with 3mm thickness and 1000mm span. This new mould has the capability of being used for in situ sampling as the tube can be directly inserted into the soil as used in recent works (Silva *et al.* 2014; Costa 2011) to directly recover samples. Moreover the PVC is a cheaper and more adaptable solution than the former acrylic U-shaped mould. Since then, the tube has been undergoing small modifications as a slightly reduction of the span and thickness. The mould has been tested with samples directly retrieved from a layer and with reconstituted specimens where the bulk density is controlled.

The applications of EMM-ARM technique to sand-cement materials have been successful, provided that the characteristics of the specimens as the bulk density or the content of the mixture are representative of the soil to test. For example a difference of  $100\text{Kg/m}^3$  can result in a difference of 0.5 GPa as in previous works (Silva *et al.* 2014).

Despite the success in the existing application of EMM-ARM to stabilized soils, there are some issues associated that still need to be addressed to improve the applicability of this methodology:

- Deviations of ambient vibration from white noise conditions, with strong contamination at certain frequency levels are a recurrent problem that brings added difficulties to the identification of the resonance frequency.
- EMM-ARM still lacks a sampling procedure that can be used on in-situ conditions. Indeed, the development of a sampler that allows the retrieving samples that represent the in-situ conditions is of utmost importance.

### 2.1.1.3 Procedure/methodology applied to stabilized soils

The latest procedure of EMM-ARM (Silva *et al.* 2013) consists in placing the freshly mixed material in a PVC tube (50mm of outside diameter and 1.5mm tick), as presented in Figure 4. The PVC tube has known geometry, mechanical properties and support conditions (normally a simply supported tube (Silva *et al.* 2013; Costa 2011). The mould can be filled whether by sampling or by placing the fresh mix into the mould by hand (here termed as ‘reconstitution’).

For a reconstituted specimen the mixture is placed inside the mould with the bottom side sealed. The soil-cement is progressively compacted in the mould with a steel rammer and the density is controlled by weighing the sample, as to achieve a target density value corresponding to in-situ conditions after compaction (Silva *et al.* 2014). For a sampled specimen the compaction is made directly on the layer and then retrieved for the mould. Either way, after being adequately filled, the mould is sealed in both extremities with wooden disks (Silva *et al.* 2014). Screws are used to assist the materialization of simply supported conditions near the extremity of the mould, as shown in Figure 4.

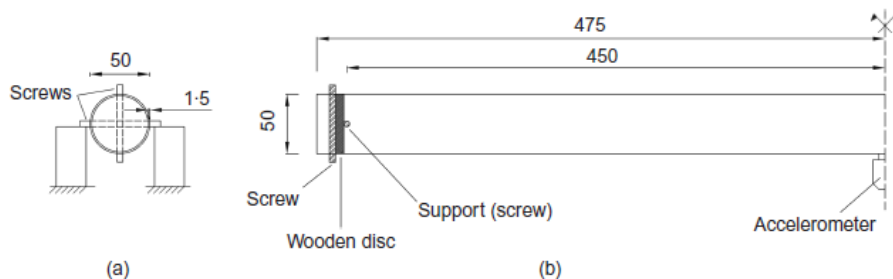


Figure 4 - Tubular PVC mould: (a) cross-section; (b) lateral view (units: mm) (Silva *et al.* 2013)

An accelerometer is attached at the bottom mid-span surface of the mould and connected to an acquisition system. The accelerometer will measure the accelerations suffered by the beam over a defined time (e.g. sets of 300 acquired at intervals of 900s).



The data is then treated using the Fast Fourier transform (FFT) following the Welch procedure (Welch 1967), thus converting data from time-domain to frequency-domain, on sets that usually comprise 2048 or 4096 points. The data processing is schematically shown in Figure 5, starting with the initial data (a) of 300s split up in overlapping segments (an overlap of 50% is used in EMM-ARM) (b). Each segment has 4096 points for a total of 73 segments are then multiplied by Hanning windows (c).

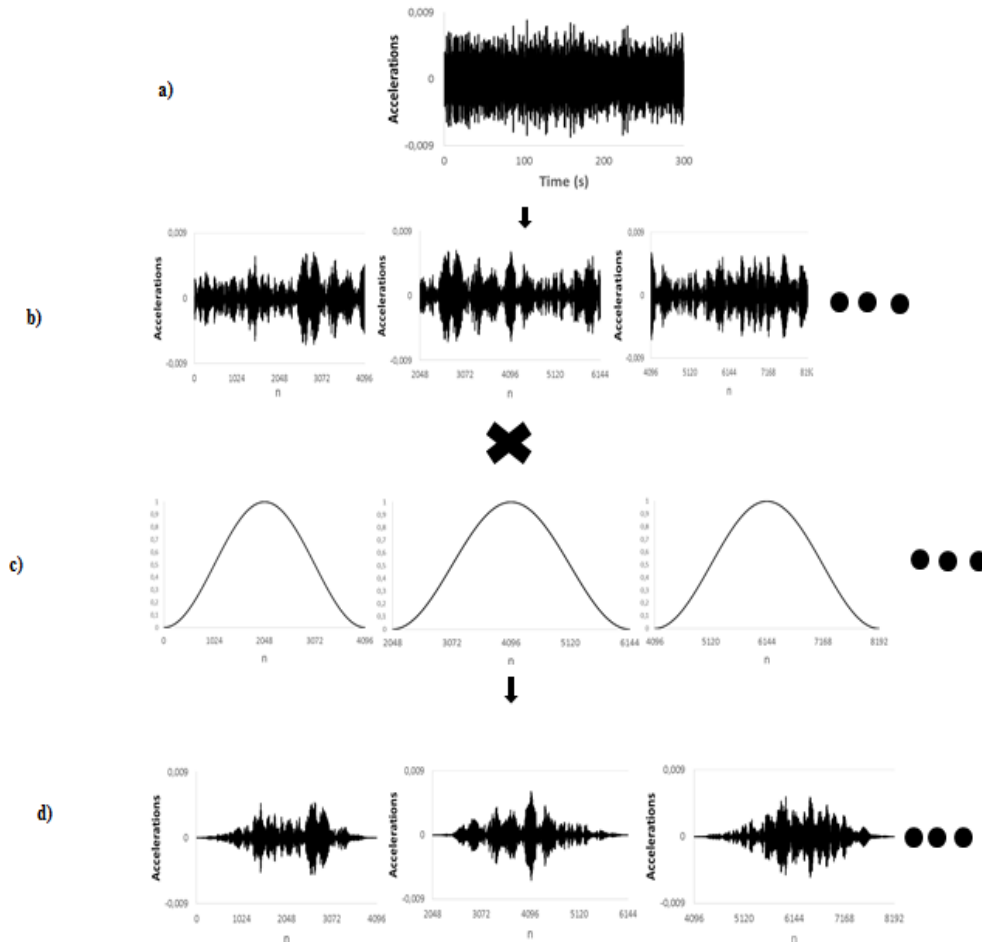


Figure 5 - The windows of Hanning with 50% overlap

The Fast Fourier Transform (FFT) is applied to each of the segments mentioned above after windowing (d), thus converting the data into the frequency domain. The Welch procedure ends by averaging of the frequency spectra obtained from all segments. A typical result can be observed in Figure 6.

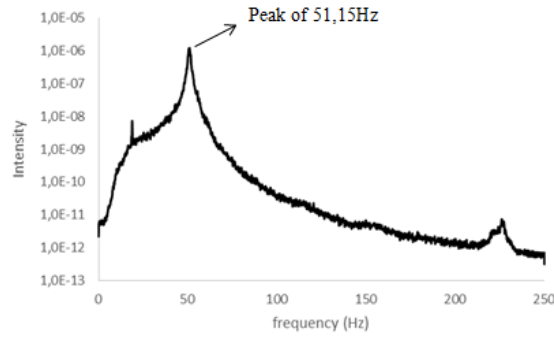


Figure 6 - Average of the FFT segments

With the spectrum in the frequency-domain, the next step is to identify the resonance frequency. The Peak Picking method, which is straightforward and robust is used for such purpose. This method is based on the assumption that for frequencies close to the resonance frequency of the structure, the dynamic response is essentially conditioned for the contribution of the resonance mode for example in Figure 6 the frequency in which the structure had more response/intensity was at 51,15 Hz (Magalhães 2012).

Following the identification of the resonance frequency it is necessary to correlate the frequency to the E-modulus of the tested material through the equation of motion. Azenha (2009) presented an equation that relates the first flexural resonance frequency ( $w$ ) with the stiffness of a simply supported beam ( $\overline{EI}$ ) with a concentrated mass at the mid-span ( $m_p$ ) and length ( $L$ ) for the case that the supports are flexible, as at the time it was not possible to assure the rigidity of the supports. Meanwhile through new experimental procedures it was possible to assure the rigidity of the supports thus the deduced equation for infinite rigidity of the supports is:

$$-\cosh(aL) w^2 m_p \sin(aL) + 2 \cos(aL) a^3 \cosh(aL) + \cos(aL) w^2 m_p \sinh(aL) = 0 \quad (1)$$

Where:

$$a = \sqrt[4]{\frac{\overline{m} w^2}{\overline{EI}}} \quad (2)$$

The scheme of the simply supported beam simulated is presented in Figure 7.

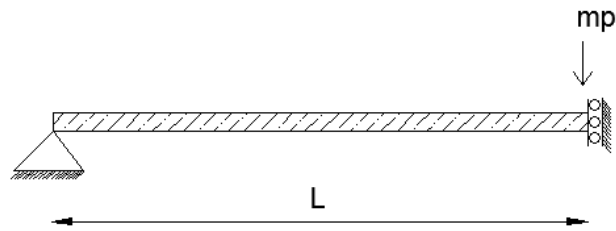


Figure 7 - Sketch of half-beam

Upon knowledge of  $(\overline{EI})$ , and based on the fact that the stiffness and inertia of the mould/specimen are known, it is possible to directly infer the E-modulus of the tested material with the following equation.

$$\overline{EI} = E_{\text{mould}}I_{\text{mould}} + E_{\text{testing material}}I_{\text{testing material}} \quad (3)$$

The process is repeated for every set at every age of the material in order to obtain the continuous curve E modulus-time.

### 2.1.2 Uniaxial compression test

The uniaxial compression test consists in applying a compression stress on the longitudinal axis of a specimen and then measures the strains normally in the range of very small to small strains. The stress is applied at a controlled speed, at each instant the stress applied and the strains locally measured by each transducer on the specimen are registered (Gomes Correia *et al.* 2006). This technique allows the performance of non-destructive tests through cycles of load and unload in which the specimen is submitted to loads in the elastic limit of the material. The Figure 8 presents a uniaxial compression test using a load cell and with LVDTs measuring the displacement.



Figure 8 - Uniaxial compression test with LVDTs mounted (Silva 2010)

The measurement of the strains requires equipment of high precision, the most common are the LVDTs (linear variable differential transformer) and the LDT's (local deformation transducer).

### 2.1.3 Bender elements

Bender Elements (BE) have many benefits that make them a desirable technology on the use on tests regarding the determination of material properties. This technique is a non-destructive way of dynamic testing on soils and can measure the stiffness parameters at a specific stress level without apply stresses or deform the specimen in order to perform the measurements. Also, it is possibly to change the frequency at which the BE is excited in order to better accommodate the material being tested and to obtain the clearest signal possible. It has multi-directional capabilities and can be incorporated in many setups - including triaxial and resonant-column tests, presenting smaller strain levels and remaining entirely in the elastic region (Marjanovic 2012) .

Shirley and Hampton (1978) were the first to measure shear wave velocity ( $V_S$ ) using bender elements. Figure 9 presents a typical schematic diagram of bender element system. Basically the system comprises of two bonded thin piezoelectric plates, which are usually coated with epoxy resin. Two such elements (transmitter and receiver) are normally placed opposite one another and the BE cantilever inserted at a small distance into the soil sample. The transmitter element distorts or bends when subjected to the voltage signal from the function generator and creates the shear waves. The shear wave travels through the specimen and causes the receiver element to vibrate and the arrival time of signal is recorded by an oscilloscope. The interval between the times of transmitted and received signal is calculated as the travel time ( $t_t$ ) of the shear wave.  $V_S$  is then calculated by

dividing the distance travelled by the shear wave over the  $t_t$  taken. The shear wave travel distance is normally considered as the distance between tip-to-tip (L<sub>tt</sub>) of BE (Brignoli *et al.* 1996). The shear modulus is calculated through:

$$G = \rho V_s^2 \quad (4)$$

Where  $\rho$  is the mass density of the medium and  $V_s$  is the velocity of the waves.

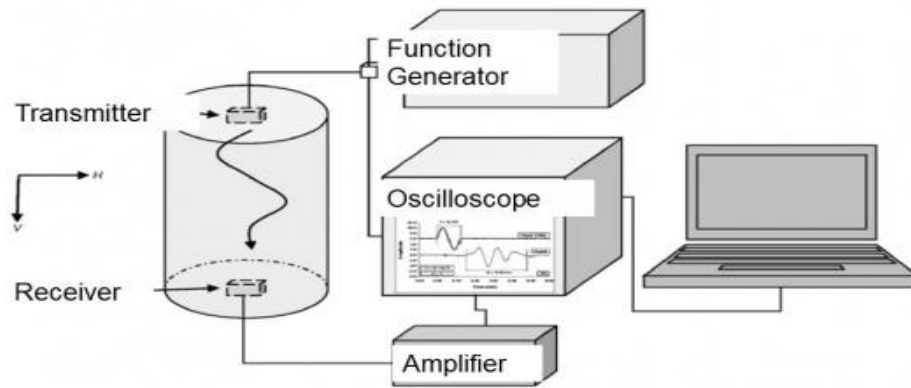


Figure 9 - Sketch of a Bender elements setup after(Alvarado & Coop 2012)

Despite allowing non-destructive tests and being a relatively cheap test there are some uncertainties on reading the results namely the distance and time of propagation of the wave.

#### 2.1.4 Ultrasonic tests

The tests through the transmission of supersonic waves are based on the theory that the speed of propagation of waves through the medium depends on the elastic properties and the density of the medium (Meyers & Chawla 2008). Thus, this technic may be used to ascertain the mechanical and physical properties of soils (Stephenson 1978) or cementitious materials (Voigt *et al.* 2006). The advantage of the technique is to be a non-destructive method. This method can use compression waves (P) and/or shear waves. The wave travels through the specimen and as in benders elements the arrival time is recorded. The interval between the times of transmitted and received signal is calculated as the travel time ( $t_t$ ) of the wave.  $V_s/V_p$  is then calculated by dividing the distance travelled by the wave over the  $t_t$  taken. If the two waves (compression and shear) are used it is possible to

ascertain the dynamic module of deformability and the Poisson's ratio through the following equations:

$$E = \frac{\rho V_s^2 (3V_p^2 - 4V_s^2)}{V_p^2 - V_s^2} \quad (5)$$

$$v = \frac{V_p^2 - 2V_s^2}{2(V_p^2 - V_s^2)} \quad (6)$$

To determine the elasticity modulus it is required to know the velocity of the two waves and as the sensors only work with one type of wave the application of the technique can become complex. Due to the transducers characteristics it is more efficient to use P waves, using just this wave, it is possible to obtain the constrained modulus M and the dynamic modulus E if the Poisson ratio is known.

$$M = \rho V_p^2 \quad (7)$$

$$E = M \frac{(1 + v)(1 - 2v)}{(1 - v)} \quad (8)$$

The application of the technique can be performed using probes, the test is easy and fast although the interpretation of the results namely identifying the exact time of the wave propagation can be problematic. The sensibility of the operator in the interpretation of the data is a matter of the utmost importance for the precision of the results. The Figure 10 shows a schematic representation of ultrasonic test setup (Yesiller *et al.* 2001).

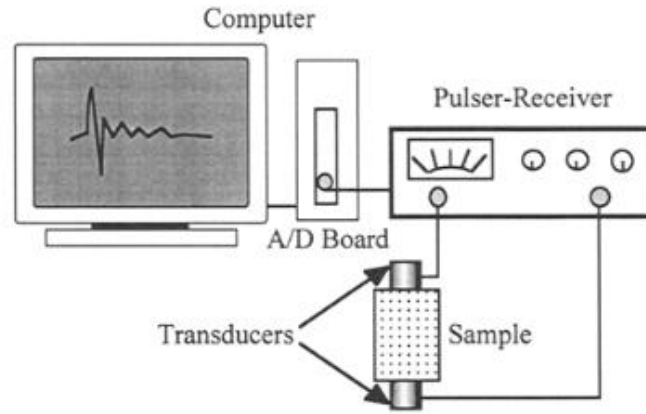


Figure 10 - Schematic Ultrasonic setup (Yesiller *et al.* 2001)

## 2.2 Field tests

### 2.2.1 Static load plate test

The Static load test plate is a technique that allows the determination of the characteristics of deformability of the layers. It is a laborious and time-consuming technique, whereby normally the number of trial is limited, not providing a statistical basis about the quality of layers (Gomes Correia *et al.* 2009). There are several testing standards, for instance AFNOR NF P94-117-1. This test has a purpose of ascertain the module of deformability under static load applied to a plate on a platform.

The test is based on the application, after a preload, of two successive cycles of loading through a plate of stiffness and diameter standardized. In the first load cycle, during the time required to stabilize the displacement of the plate it should be maintained an average stress on the plate of 0,25 MP. During the second load cycle the average stress on the plate should be 0,20 MPa and, as in the first period, the unload should be performed only after stabilization of deflection. The strain modulus,  $E_{v2}$ , is calculated for the second load period by the Boussinesq solution, using the secant method according to the equation for rigid plates (Gomes Correia *et al.* 2009):

$$E_{v2} = \frac{\pi}{2} (1 - \nu)^2 \frac{p \cdot r}{z_2} \quad (9)$$

Where  $\nu$  is the Poisson ratio,  $p$  is the pressure on the plate,  $r$  is the radius and  $z_2$  is the displacement of the plate.

In Figure 11 is a set up by the North Carolina Department Of Transportation.



Figure 11 - Load Cell and Plate Set Up from NCDOT

### 2.2.2 Light Weight Deflectometer

The Light Weight Deflectometer or LWD is a portable equipment to determine, “in situ”, the dynamic modulus of deformation ( $E$ ). The principle of working is based on the fall of a mass from a defined height over a rigid circular loading plate. The impulse to inflict load is measured through a load cell and the displacement through geophones. After measuring the displacement of the plate and the charge applied it is possible to determine the strain modulus  $E_{LFW D}$ , through Boussinesq solution (Gomes Correia *et al.* 2009) using the following equation:

$$E_{LFW D} = \frac{k \cdot (1 - \nu)^2 \cdot \sigma \cdot R}{\delta_c} \quad (10)$$

In which  $k$  is equal to  $\pi/2$  or  $2$ , to rigid or flexible plates, respectively,  $\delta_c$  is the displacement on the center of the plate,  $\sigma$  is the tension applied and  $R$  is the radius of the plate. The Figure 12 shows the equipment normally used in this test.



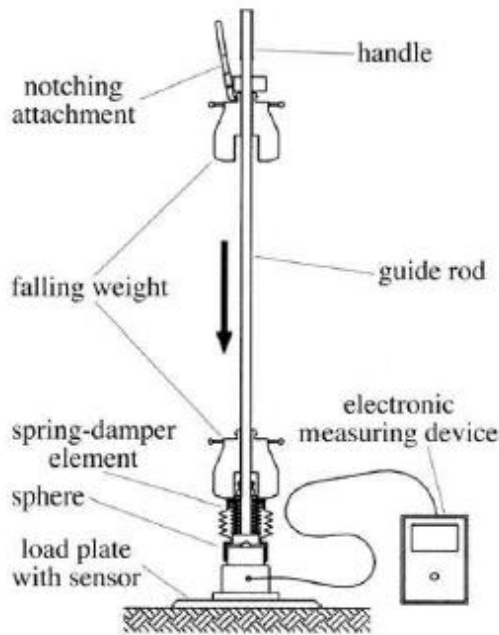


Figure 12 - Light Weight Deflectometer (Adam & Adam 2003)

### 2.2.3 Humbolt stiffness gauge

Humboldt Stiffness Gauge also called as “geogauge” is an equipment, used “in situ” that through non-destructive testing allows the determination of the stiffness of the layer and the modulus of deformability ( $E$ ). The geogauge, as presented in Figure 13, can be used in different materials as soils or treated soils. This equipment has a rigid ring that contacts the soil and an electromechanical vibrator that produces frequencies in the range between 100Hz and 196 Hz, with increments of 4 Hz, generating 25 specific frequencies and forces of about 9N. This vibration force produces small deflections that are measured by the geogauge. A microprocessor calculates the stiffness ( $k$ ) for each frequency and presents the average value. The stiffness can then be converted into soil strain modulus ( $E_{SSG}$ ) by the equation (Gomes Correia *et al.* 2009):

$$E_{SSG} = \frac{k \cdot (1 - \nu)^2}{1,77 \cdot R} \quad (11)$$

Where  $k$  is the stiffness presented by the geogauge,  $\nu$  the Poisson ratio and  $R$  the radius of the rigid ring.

Each test takes about 75 seconds and according to the National Cooperative Highway Research Program the results will have high variability when testing non-cohesive, well-graded sands or similar soils and the modulus readings from the gauge represent an equivalent modulus for the upper 25,5 cm to 30,5 cm of the layer. Therefore the gauge should not be used to test thin (less than 101,6cm) or thick (greater than 30,5 cm) layers without proper material calibration adjustments.



Figure 13 - Humbolt equipment

### 2.3 E-modulus vs strain level

The E value measured by each test is influenced by several parameters such as the strain amplitude during the test, the mean effective stress, the void ratio, the preconsolidation stress or the effective material strength (Houlsby *et al.* 2005;Benz 2007).

Particularly the strain level that the soil sustains during the E measurement test is highly influential on the elasticity modulus value. The effect of the strain level on the Elasticity modulus value can be simulated through some constitutive models. For instance the Simpson brick model is a widely used model in which a strain level step corresponds to a determined elasticity modulus (Benz 2007). This model gives an approximation of the real stiffness-strain curve as can be seen in the Figure 14.

Gomes Correia *et al.* (2004) through numerical simulations of the Menard pressuremeter test (PMT) and plate load test (PLT) showed the modulus as function of strain level. Figure 15 shows the results.

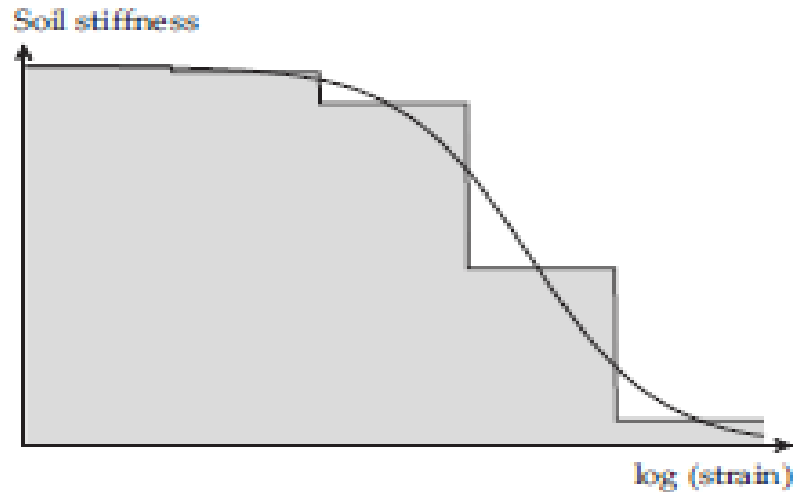


Figure 14 - Steps of the Simpson model compared with the real stiffness-strain curve (Benz 2007)

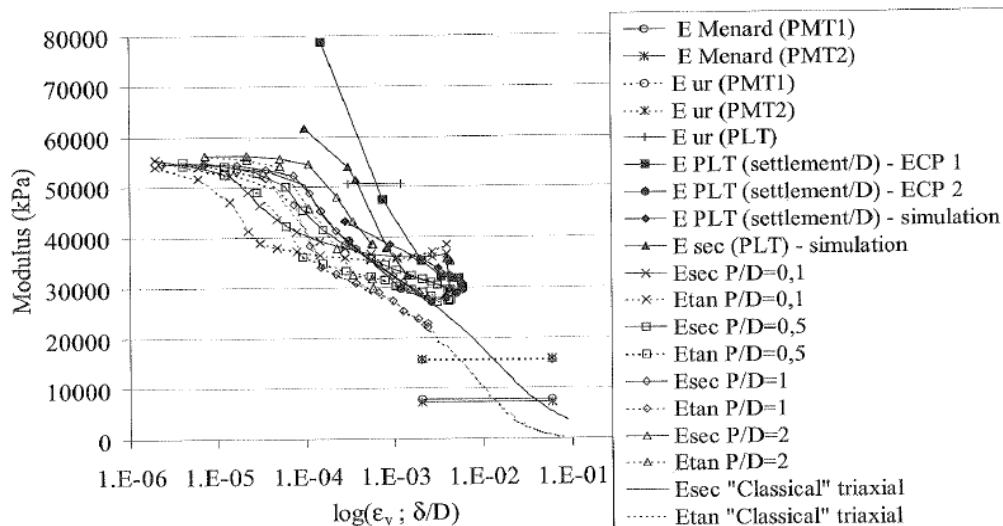


Figure 15 - Moduli as a function of strain level for various numerical simulations and test analysis

As can be seen in the Figure 15 the numerical tests carried out by Gomes Correia *et al.* (2004) showed the degradation of the modulus with the increase of the strain on the soil. Moreover the interpretation of the tests was proved as being influential on the results for instance the secant modulus of the unload-reload cycle of the Menard test is around 2.2 times the tangent modulus.(Gomes Correia *et al.* 2004).

Thereby each e modulus obtained is used in a different manner. When the strain level have a value below 0,5% it is used for deformation analysis for values above it is used for

ultimate state analysis such as bearing capacity or stability analysis (Gomes Correia *et al.* 2004).

## 2.4 Overall summary table

Table 1 summarizes the presented methods of elasticity modulus assessment:

Table 1 - Assessment tests summary

Test	Main measured parameter	Strain Level	Remarks
EMM-ARM	E -small strain stiffness	$<10^{-6}$	Allows the automatic continuous measurement since early ages
UCC	E -small strain stiffness	$<5 \times 10^{-5}$	Generally used Limited use at early ages
Benders	G0-Small strain Shear modulus	$<1 \times 10^{-6}$	Easy to use but there are some doubts on reading the results
US	M Constrained modulus E Dynamic Modulus	$10^{-6}\%$	Same as benders
SLP	$E_{v2}$ strain modulus	$10^{-3}\%$	Time consuming and costly
LWD	$E_{LFWD}$ strain modulus	Between $10^{-3}$ and $10^{-4}$	More portable than the static plate
Humbolt	$E_{SSG}$ soil strain modulus	Reported as small	Fast but depth limited

In this dissertation it will be used EMM-ARM and UCC tests. Therefore the parameter assessed will be the small-strain stiffness. For small strains the variation of the modulus is minimal and the values can be directly compared.

### 3 DEVELOPMENT OF SAMPLER

#### 3.1 Sampling: general considerations

In order to directly characterize the soil of a given layer, direct sampling of the soil for laboratory testing can be considered as highly recommended. Samples retrieved from the soil can be grouped in 3 categories: non-representative samples that are unsuitable for laboratory testing, representative samples that contain all mineral constituents of the layer without contamination of other material but might not be representative of the state of water content or micro-structure (Nagaraj 1993) and undisturbed samples that are those which are obtained with the minimum disturbance to the in-situ conditions (Marcuson III & Franklin 1979). The disturbance can occur during drilling, sampling, transportation, storage or preparation for testing. According to Clayton *et al.* (1995), the mechanisms associated with disturbance can be:

- changes in stress conditions;
- mechanical deformation;
- changes in water content and voids ratio;
- chemical changes.

To assure that the characteristics of the specimens are representative of those found in the field, collecting undisturbed samples is a matter of the utmost importance. That is especially the case when evaluating the mechanical properties of the soil such as the deformation modulus.

There are several techniques for soil sampling, with the most common being block sampling and tube sampling.

#### 3.2 Block sampling

The method that involves less disturbance, due to the fact that the soil does not suffer shear stress, is the block sampling and is considered the bench-mark (Siddique *et al.* 2006).

A block sample can be retrieved from a pit/exposure by trimming the soil with a sharp knife or retrieved from a borehole using a specific sampler as the Sherbrooke sampler. Excavation of a pit can be an economical way of acquiring a very detailed record of the complex soils conditions although in some conditions such as in normally and lightly overconsolidated clays, the excavation of a pit or shaft with more than a few meters is often impossible (Clayton *et al.* 1995). The Sherbrooke sampler can overcome that problem because it only requires a borehole of 40 cm diameter. The sampler has a trimming mechanism that cuts the soil. In the Figure 16 is the apparatus proposed by Lefebvre & Poulin (1979) for retrieving block samples.

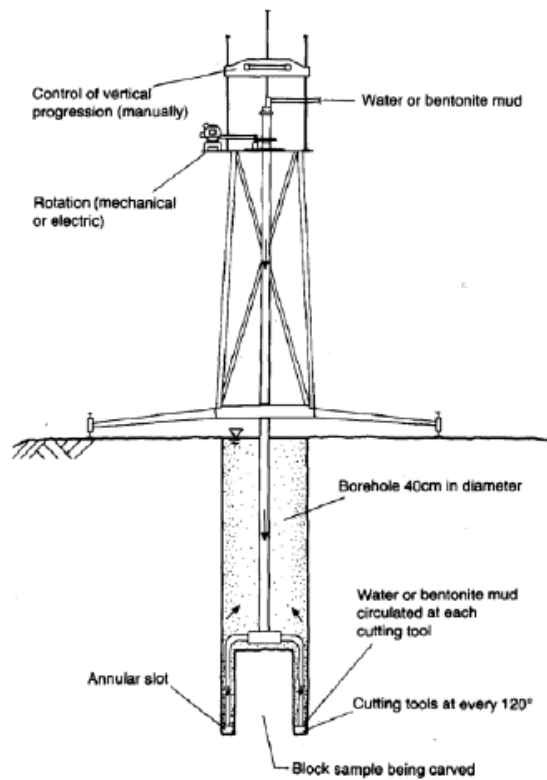


Figure 16 - Schematic diagram of the Sherbrooke down-hole block sampler (Lefebvre & Poulin 1979)

In this technique the sampler is lowered to the base of the hole using a mechanically-induced or electrically-induced rotation. A cylinder of about 250mm in diameter is carved out by 3 circumferential blades at the base (Clayton *et al.* 1995). Despite allowing high quality samples the process is complex and time-consuming.

### 3.3 Tube Samplers

Tube samplers are driven or rotated into the soil to retrieve a sample. Tube sampling is an easier and less time-consuming way of collecting samples, as compared to block sampling. For such reasons, it is the most widespread technique (Clayton *et al.* 1995). A tube sampler can be retrieved from pits/exposures or boreholes, and in some cases directly driven or rotated into the soil.

#### 3.3.1 Design considerations

The characteristics of the tube samplers are related to the quality of the sample. Therefore it is important to consider its dimensions in the selection of the tube sampler to further obtain better sampling quality. In the analysis of samplers quality, the block sampling is normally used as the benchmark because such method is known to induce very small levels of disturbance. Figure 17 shows the geometrical data that is used to characterize a tube sampler. In which  $R$  is the external radius,  $R_1$  is the radius at the bottom edge,  $R_2$  the radius along the sampler,  $H_1/H_2$  the internal/external height along the cutting edge,  $\alpha/\beta$  the external/internal cutting angle and  $t$  the thickness.

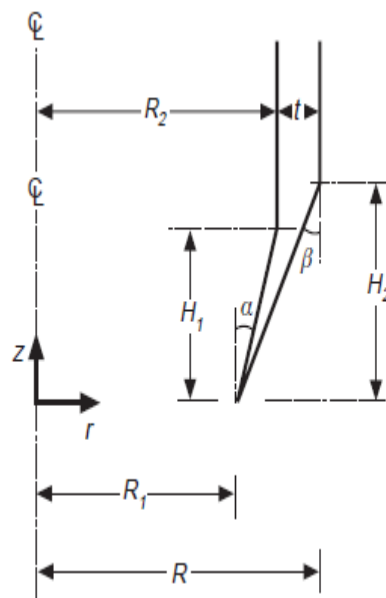


Figure 17 - Dimensions of a tube sampler (Clayton *et al.* 1998)

The analysis of the expected performance of a given tube sampler can be made through evaluation of geometrical ratios. The most widespread index is the ratio of area (AR) that relates the inside diameter in the cutting edge with the outside diameter (Clayton *et al.* 1998; Siddique *et al.* 2006).

$$AR = \frac{R^2 - R1^2}{R1^2} \quad (12)$$

As described by Hvorslev (1949) the ratio is a relation between the volume of displaced soil and the volume of the sample itself. To compare the effect of AR on sample quality Siddique *et al.* (2006) performed tests in Bangladesh clays in which the AR of tube sampler was varied whereas the cutting edges and length were kept constants. Figure 18 presents the results of  $\varepsilon$  (strain),  $s$  (shear strength) and  $E$  (initial tangent modulus), which were normalized to the corresponding values obtained through the block sampling technique.

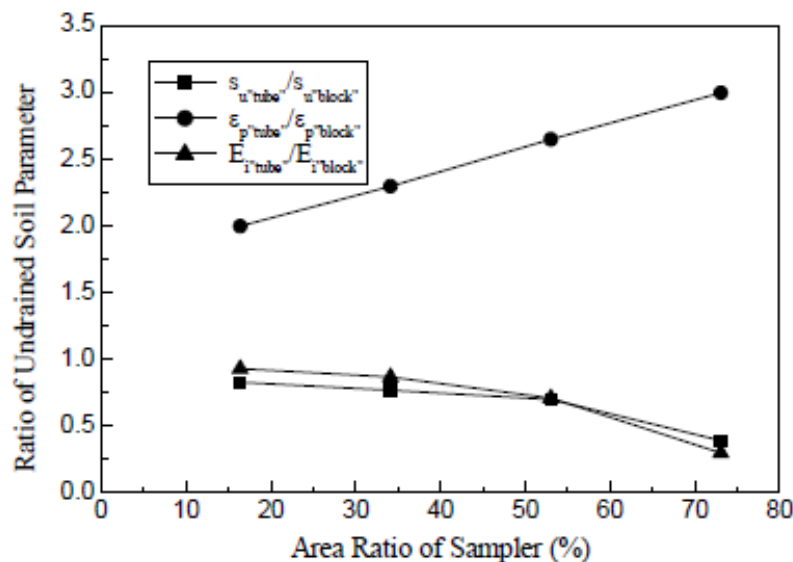


Figure 18 - Influence of AR in sample quality (Siddique *et al.* 2006)

It can be observed that an increase of AR induces an increase of the disturbance of the sample namely an increase of strain  $\varepsilon$  and a decrease of shear strength and initial tangent modulus  $E$ . The shear strength and the initial modulus in tube sampling is inferior than in block sampling as its value is below 1 regardless the AR. Thus as expected the block sampler gives the best sample. As AR is reduced, so do the changes in stress condition and the mechanical disturbance of the soil structure (Briaud 2013). Siddique (1990) recommends to use an AR of less than 10%.

Another parameter used to evaluate the sample disturbance is the relation external diameter-thickness ( $R/t$ ) of the sampler. Through numerical analysis, Clayton *et al.* (1998)



were able to estimate the strain caused by sampling along the sampler for different R/t values, as presented in Figure 19 ( in the figure R is named as B):

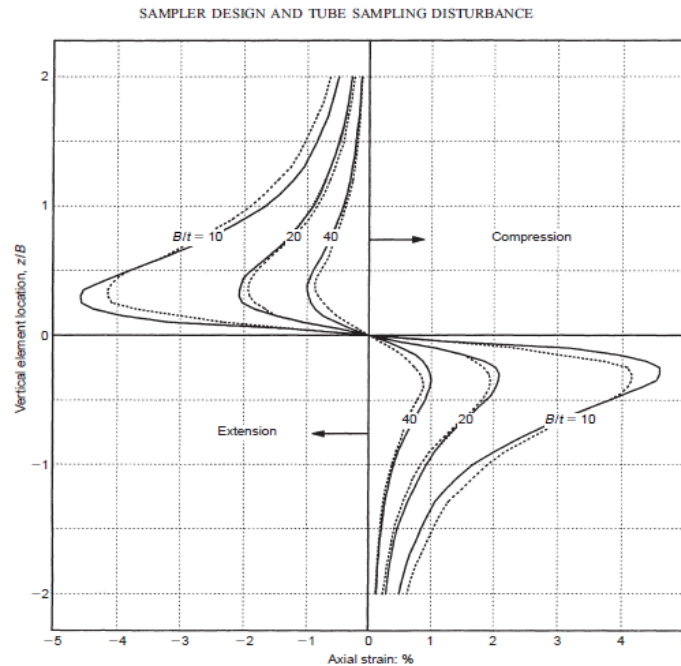


Figure 19 - Analytical solutions for axial strain history at the center-line of the sampler for different B/t ratio (Clayton *et al.* 1998)

As can be seen in Figure 19, higher values of R/t correspond better the sample quality. The maximum strain can be obtained by  $0,385 t/R$ , the simplicity and precision of this equation means that can be used in a practical and simple way to estimate disturbances of tube samplers a R/t between 40 and 47 is used in United States practice (Baligh *et al.* 1987).

Another parameter of importance is the Inside Clearance Ratio that is produced by swaging the cutting edge of the tube, creating a different radius at the bottom edge of the tube ( $R_1$ ) and at the inside of the tube ( $R_2$ ).

$$ICR = \frac{R_2^2 - R_1^2}{R_1^2} \quad (13)$$

The ICR reduces the friction between the sample and the inside wall of the tube during sampling (Marcuson III & Franklin 1979) , thus has been introduced in the tube samplers to prevent jamming.

Although it minimizes the shear stresses between the soil and the inside of the tube, it allows lateral expansion of the soil once in the tube, thus the ICR increases the sample

disturbance. Clayton *et al* (1998) recommended an ICR between 0,4% and 1,5% and Kelleher *et al.*(2008) recommended an ICR inferior to 1% to maximize sample quality.

The design of the cutting edges affects the sample quality. An increase of the outside cutting edge angle (OCA) or the inside cutting edge angle (ICA) means an increase of the strains (Clayton *et al.* 1995; Siddique 1990).

$$ICA(\alpha) = \tan^{-1} \frac{R2 - R1}{H1} \quad (14)$$

$$OCA(\beta) = \tan^{-1} \frac{R - R1}{H2} \quad (15)$$

Tanaka (2008) concluded that a small cutting edge angle allows better sample quality than big angles. Siddique (1990) recommended that the samplers should have a small OCA, preferably not more than 5° and an ICA of 1° to 1.5°.

A reduction of the overall cutting edge (OCE) can be used to counter the effects of a high area of ratio (AR) (Clayton *et al.* 1998). The International Society for Soil Mechanics and Foundation Engineering's Subcommittee on Problems and Practices of Soil Sampling (1965) suggested combinations of AR and OCE for 75mm samplers. The Table 2 shows the proposal combinations.

Table 2 - Combinations of AR and OCE

AR: %	Overall cutting edge taper angle: °
5	15
10	12
20	9
40	5
80	4

### 3.3.2 Drive samplers

Drive samplers are samplers that are pushed or driven into the soil without rotation generally cutting the soil with a sharp cutting edge at their base. The volume of soil corresponding to the thickness of the sampler is moved to the surrounding soil which is either compressed or compacted (Clayton *et al.* 1995). The characteristics of the sampler depend on the soil to test. Drive samplers can be classified according to their thickness, to the presence of extremity opening (open-drive samplers) or to the inclusion of a piston

(Clayton *et al.* 1995). In this dissertation they are divided in 3 groups: thin-walled (open-drive), thick-walled (open-drive) and piston samplers (thin and thick-walled).

### 3.3.2.1 Thin-walled drive samplers

The Shelby tube or thin wall tube was introduced in the United States in the 1930's. It has an AR of 11.7% and a cutting angle of about 44°. A further improvement was made in the modified Shelby with an AR of 4.3% and an angle of 5° (Landon 2007). Their geometrical characteristics induce very low disturbance to the soil. Therefore, these samplers are mainly used with clays and silts and retrieve undisturbed samples suited to many quality laboratory tests (Briaud 2013). This sampler has the disadvantage of being easily damaged. Figure 20 shows the Shelby tube available at the University of Minho.



Figure 20 - Shelby tube available at the University of Minho

### 3.3.2.2 Thick-walled drive samplers

A thick-walled sampler is a sampler whose AR is greater than 20%. Although is a more expensive sampler than a thin-walled, has more strength and is more suitable for harshest soils. The sample retrieved is usually more disturbed than in thinner samplers.

The British U100 is one of the most common thick-walled samplers. The sampler is driven into the ground through a slide-hammer. Between the sampler and the hammer is a drive head that contains a valve which allows the release of the air while the tube is introduced into the soil and helps to held the sample in place when it is being withdrawn (Bell 2004). Figure 21 presents a scheme of the U100 sampler. Both the drive head and the cutting shoe

are screwed to the sampler. The sample retrieved has a nominal radius of 100 mm and a length of 450mm. The AR of the sampler is 27% and the OCA above 20. The value of the area ratio is increased when a liner is used (40%) (Clayton *et al.* 1995). These values of AR and OCA are very high therefore the expectable sample is of poor quality.

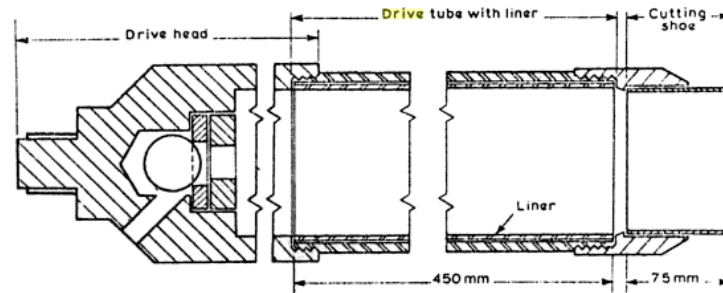


Figure 21 - Scheme of the U100 sampler (Bell 2004)

Split barrel samplers are thick-walled samplers which are divided into two halves lengthwise. During the introduction into the soil these are held together by the shoe and head which are screwed on to each end (Clayton *et al.* 1995). This allows to easily examine and extract samples from the sampler itself as the soil can be retrieved when the sampler is opened. The sampler used during the SPT (shown in Figure 22) and the modified California sampler are examples of split barrel samplers.



Figure 22 - SPT Sampler

This type of sampler has a very high area ratio, it is used primarily with sand and gravels, and it has been acknowledged to collect disturbed samples well suited for soil identification and classification purposes (Briaud 2013).

### 3.3.2.3 Piston drive samplers

These samplers contrary to the open-drive samplers have the lower end of the tube closed with a piston which can be held stationary, withdrawn or left free to allow flexibility of operation (Nagaraj 1993).

The piston can contribute for a good quality in sampling. Samplers can have a piston in order to: prevent soil of entering in the sampler before the desired collecting position is achieved, to reduce sample losses, to reduce the entry of soil in excess in the tube during the initial stage of driving, to increase the acceptable ratio length / diameter ratios (Clayton *et al.* 1995) and to serve as an effective check valve (Nagaraj 1993). The piston can be used in both thin and thick walled tubes, permitting to obtain high quality samples.

There are several ways of held a piston in a sampler. The Geonor sampler/piston is a widespread solution that comprises a thin walled sampler which uses a stationary piston as presented in Figure 23. In this case the sampler is lowered to the level at which sampling is to start (if a borehole is used), the piston rod is then fixed to the drilling rod and the sampler goes down while the piston stays at the initial position (Clayton *et al.* 1995) in other words the piston is placed at the bottom of the sampler and stays stationary while the sampler slides down to collect the sample. When the sampler is full the piston and the sampler are pulled.

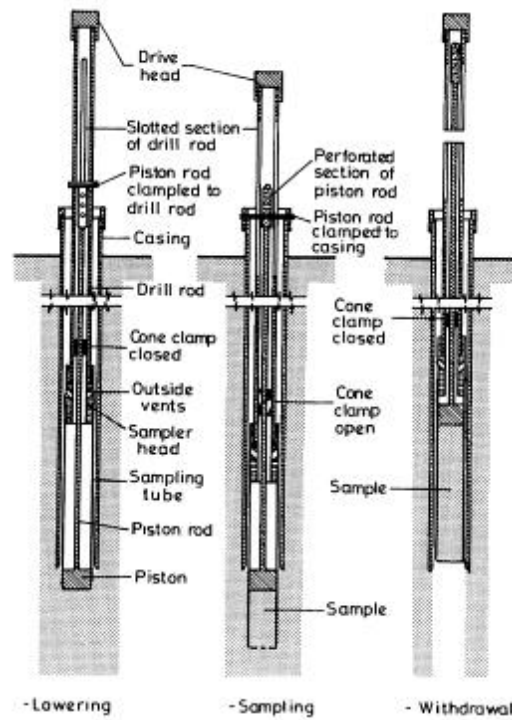


Figure 23 - Sampler with stationary piston (Nagaraj 1993)

This sampler allows to collect undisturbed samples of soft to stiff cohesive soils (Fang 1990). It also allows a good sample quality in loose/media dense sands if the hole is filled with drilling mud (Marcuson III & Franklin 1979).

There are several samplers with stationary piston, such as the Japanese sampler of 75mm with stationary piston, that has an AR of 7.5% allows samples with slightly inferior quality to that obtained by the Sherbrooke sampler (Tanaka 2008).

The Osterberg thin-walled hydraulic piston sampler, presented in Figure 24, has a low AR of 6% and uses two pistons.

The operation mode is similar to the stationary piston as one of the pistons (fixed piston) is held at the starting ground of sampling while the sampler goes down, moreover this sampler has one piston (floating piston) that goes down the tube by hydraulic pressure applied at ground level (Clayton *et al.* 1995). The sampler cannot be over-pushed since the push stops when the moving piston contacts the fixed piston (Fang 1990).

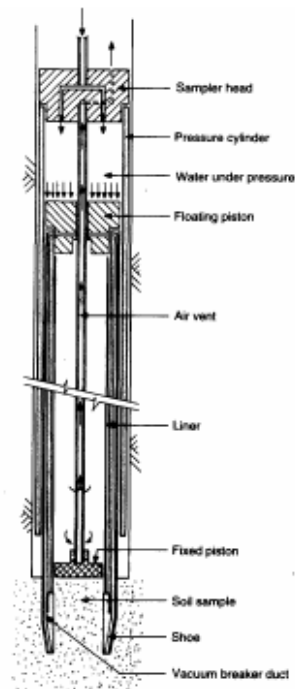


Figure 24 - Osterberg hydraulic piston sampler (Osterberg 1973)

According to Raymond (1977) this sampler is suitable to sensitive clays. Hunt (2005) recommended this sampler for very soft to firm cohesive soils. Marcuson III & Franklin (1979) pointed out that with this sampler it is not possible to limit the sample length.

### 3.3.3 Rotary Samplers

The rotary drilling uses the rotation combined with a downward force on the material and allows retrieving undisturbed samples of rocks. The rotary samplers can be applied to rocks and soils, but are more easily used in intact rocks than in fractured rocks and soils (Clayton *et al.* 1995).

The simplest form of a rotary corebarrel consists, as presented in Figure 25a, of a single tube with a coring bit at its lower edge which is loaded and rotated while a pressurized fluid passes around the bit (Clayton *et al.* 1995). In drive sampling the soil displaced by the walls of the sampler is moved to its vicinities but in the rotary samplers the material is ground up and removed by air, circulating water, or by a drill fluid (Nagaraj 1993). Samples collected with a single tube corebarrel may experience some disturbances due to torsion, swelling or contamination by the drilling fluid (Murthy 2002). The modern corebarrels have two tubes, an outer tube that rotates and an inner tube that remains

stationary. Normally the inner tubes are provided with a swivel head that prevents the core from rotating and eroding (Nagaraj 1993).

There are also the barrels of triple tube, as the Denison corebarrel presented in Figure 25b, in which a liner is inserted inside to facilitate the storage of the sample, similarly to the case of drive samplers.

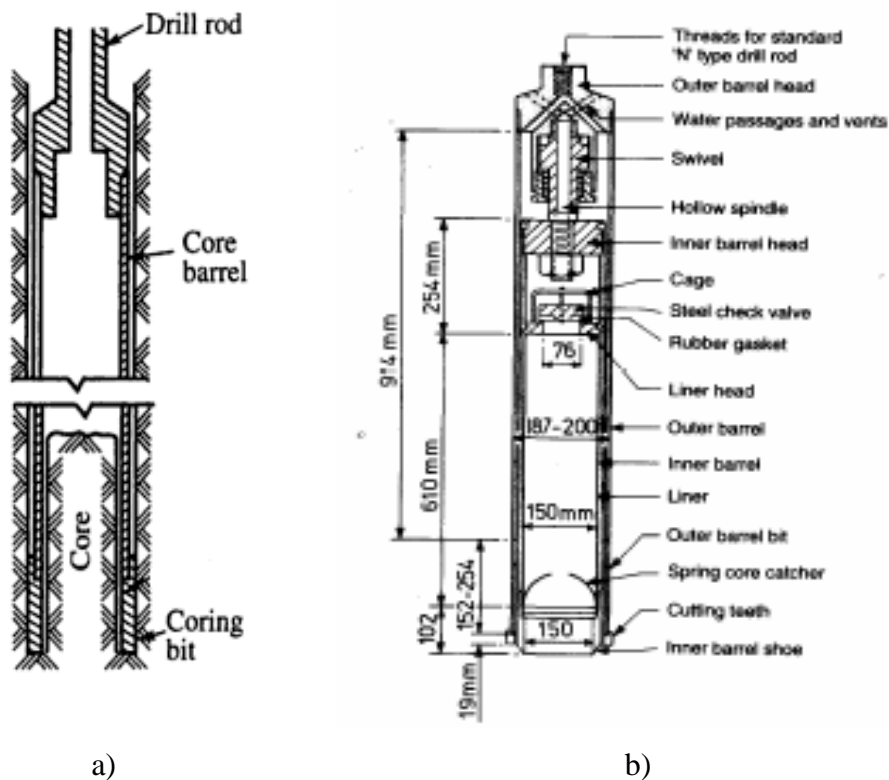


Figure 25 - a) Single tube corebarrel (Murthy 2002) b) Denison triple-tube corebarrel (Johnson 1940)

The quality of the samples retrieved by the rotary samplers depends on the material generally takes good samples but is not suitable for loose cohesionless soils and soft cohesive soils (Marcuson III & Franklin 1979).

### 3.4 Sample driving techniques

Driving a sampler into the soil requires a load on the sampler. The way the load is transmitted to the sampler will affect the sample quality. In fact, the speed and continuity



of the motion with which the sampler is forced into the soil have a manifest influence on the disturbance of the retrieved sample (Nagaraj 1993).

The sampler can be driven through blows or continuous pushing. Hvorslev (1949) pointed out some driving methods presented in Table 3.

Table 3 - Hvorslev's driving methods as in (Nagaraj 1993)

Mode	Method	Nature of movement	Remarks
Hammering	Repeated blows of a drop hammer	Intermittent fast motion	Simple but causes disturbance
Jacking	Levers or short commercial jacks	Intermittent slow motion	Reaction frame is required, some disturbance possible
Pushing	Steady force without any interruption	Continuous uniform motion	Simple, disturbance mainly due to inside friction
Single blow	Blow of a heavy drop hammer	Continuous fast motion	Simple, relatively less disturbance to samples
Shooting	Force generated by explosives	Continuous very fast motion	Desirable, method is relatively involved, least disturbance to samples

The method that induces highest disturbance to the soil is the one based on blows of a hammer, whereas the method that is less disturbing for the soil is pushing the sampler into the ground at a high and constant speed (Terzaghi & Peck 1948).

When the sampler is hammered into the soil, under each blow the sampling tube advances downward, then rebounds slightly. This upward rebound action stresses the soil at the bottom of the sampler in tension and often causes separations. This tension creates a series of tensile fractures/discontinuities between zones of compression (Rogers 2006). Figure 26 shows the contrast between hammering and pushing the sampler into the soil.

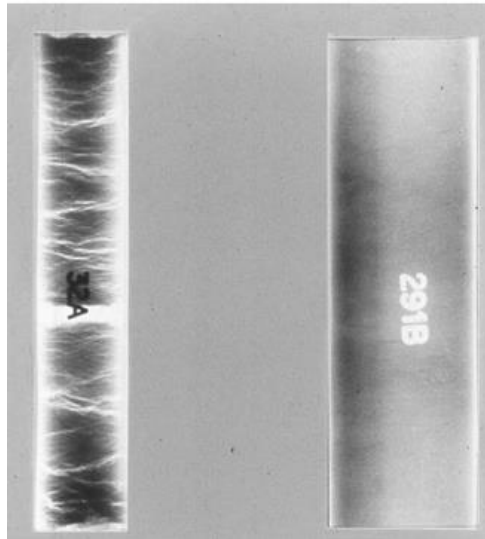


Figure 26 - X-ray photographs of sampling by hammering (left) and pushed (right) (Briaud 2013)

Hammering is shown in Figure 27, where a photo of the application of the slide hammer can be seen. In spite of being an easy and cheap method it results in poor quality samples, as being a hammering-based method. Pushing is considered the best practical method: with the support of instrumentation (load cell) and a controlled actuator, it is possible to supply a steady downwards force. Indeed, most experienced geotechnical engineers favour this method (Rogers 2006). In any case the rotation of the sampler for downward movement needs to be avoided to prevent disturbance to the soil (Nagaraj 1993).



Figure 27 - Slide hammer (Hmtri 1997)

### 3.5 Summary of sampler types

The Table 4 summarizes the samplers described in this chapter.

Table 4 - Summary of the samplers

Sampler	Main characteristics	Better Suitable for:	Typical Penetration technique
Sherbrook	Retrieves block samples High quality samples The sampling process is complex and time-consuming	Best samples in cohesive or cohesionless soils	The sampler carves the soil with circumferential blades
Thin-walled (Shelby)	Low area of ratio Simple process Good quality samples Easily damaged in hard soils	Cohesive soils	The sampler is pushed into the soil
Thick-walled	High area of ratio Less quality when compared with thin-walled	Gravel or stony soils	Normally hammered into the soil
Stationary-piston-	The piston prevents the entry of soil before the sampler reaches de target position High quality samples compared with Shelby	Soft to stiff cohesive soils	Pushed into the soil with continuous steady stroke
Hydraulic-Piston (Osterberg)	Hydraulic pressure activates the sampler High quality samples compared with Shelby Not possible to limit sample lenght	Sensitive Clays Very soft to firm cohesive soils	The hydraulic pressure pushes the sampler into the soil.
Rotary (Denison)	Have an inner tube, an outer tube and a liner. The soil displaced by the walls of the sampler is ground up.	Rocks Stiff soils	Rotation combined with downward force

The EMM-ARM methodology needs a sampler to retrieve samples immediately after compaction. At that point hardening on soil has an insignificant impact but the strength of the mixture varies with the soil. Thereby the EMM-ARM sampler should be a thick-walled sampler but keeping the AR within acceptable values in order to be sufficiently resistant to perform sampling on harder soils and to allow the retrieve of good quality samples.

### 3.6 Sampling for EMM-ARM: existing procedures

Sampling for EMM-ARM has been attempted in the past with two distinct methods (Silva *et al.* 2014).

The first method mentioned above consisted in using a prismatic wooden sampler containing a prismatic mould (acrylic) (Silva *et al.* 2014). The mould which can be seen in Figure 28 was composed by 4 polycarbonate plates connected to each other by screws allowing full disassembly after testing. In order to accommodate the screwed connections, the side plates had a larger thickness (8 mm) than the other plates of the mould (3 mm) (Silva *et al.* 2014). The assembled mould had an inner cross-section of 40 mm×40 mm and a length of 900mm. The lateral plates of this mould were used as a liner in a wooden sampler. Contrary to the majority of the samplers, this sampler had one of its largest surfaces open.

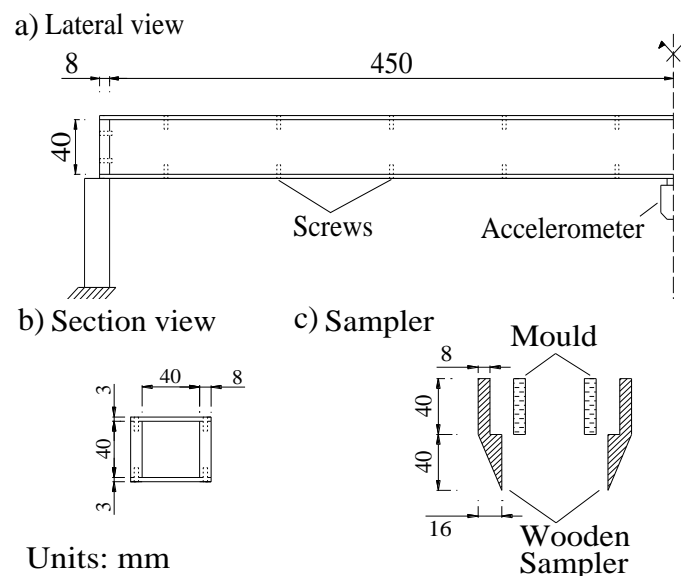


Figure 28 - Prismatic mould: a) Lateral view; b) cross-section; c) scheme of the set sampler / mould (Silva *et al.* 2014)

The collection of samples followed the procedure presented in Figure 29. The process consisted in applying a downward force (with a jack-hammer) on the sampler (Figure 29a,b). Small quantities of the material around the sampler were removed afterwards (Figure 29c). The downward force was then applied again, and stages a-c were repeated until the sample exceeded the top side of the mould Figure 29-d. The material in excess was then removed and the mould assembled Figure 29 (e and f).

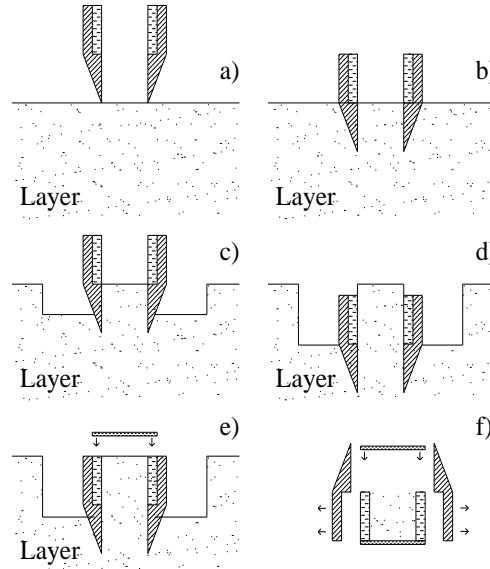


Figure 29 - Phases of the sampling process with the prismatic mould (Silva *et al.* 2014)

The wood is not the best material to compose a sampler due to the wood deformation and a stiffer material as steel should be used.

The fact that the mould was closed with the sample inside (Figure 29e and f) may have caused some disturbances because the polycarbonate plates leaned against the material and and the tighten screws caused undesired movements.

The sampler was driven into the soil in phases instead of a one-time continuous movement and that may have induced disturbance.

In this pilot application it was also used simultaneously a PVC tube with the dimensions presented in Figure 4 of Chapter 2 as both a sampler and a mould. The penetrating edge of the tube was sharpened to ease its entry into the soil. As it is shown in Figure 30: the driving sampler was initially hand pushed into the soil. However, near the end of the sampling process, the force necessary for driving increased significantly, and some hammering was needed. To recover the sampler, the surrounding soil was removed. After retrieving the sampler, the PVC tube with the material inside was then tested.

The results obtained with the PVC mould were better than the results of the prismatic mould because there were more coherent results when comparing with the UCC tests. The bulk density of the PVC sample (1884Kg/m<sup>3</sup>) was more representative of the layer(1850Kg/m<sup>3</sup>) than the prismatic sample (1982Kg/m<sup>3</sup>) this happened due to an overcompaction during the stages of sampling which caused a high value of density in the material of the prismatic mould (Silva *et al.* 2014).



Figure 30 - Details of the sampling with the PVC tube (Costa 2011)

Despite the good area of ratio of the PVC tube, the low stiffness/strength of this material may raise robustness issues in driving the sampler into the soil, as the PVC might be damaged during the sampling process. The PVC tube could be used in the inside of a stronger material that would protect the PVC during sampling and then be used as a mould for the EMM-ARM test.

### 3.7 Proposed sampler and driving technique

In order to overcome the difficulties encountered with the previous samplers for EMM-ARM testing, additional efforts were done in order to develop a new sampler of better performance. The EN 1997-2(EC7) recommends that for tests which purpose is the determination of the stiffness, the testing sample should be undisturbed.

The new sampler needed to assure some requirements for a good sampling process so that the posterior application of the EMM-ARM technique was guaranteed:

- the sampler needed to have the capability to accommodate a PVC liner that after sampling could be easily removed and used in the EMM-ARM experiment;

- the length of the sampler needed to be slightly bigger than the PVC to create a cutting angle to ease the entry of the sampler into the soil and limited to reasonable levels to assure an easy maneuverability;
- to reduce costs the dimensions of the PVC tube and of the steel used for the sampler were restricted to commercial sizes;
- the PVC tube should maintain some slenderness to keep the resonance frequencies of the composite beam from passing acceptable levels because the identification of the resonance frequency for much higher values can be harder;
- the ratios used for classifying samplers such as the ratio of area(AR) or the overall cutting edge should follow the state of art for the retrieving of undisturbed samples.

The proposal sampler was a thick-walled sampler made of steel that had an inside diameter of 51mm and 2mm thick that was capable to accommodate the 50mm PVC tube as a liner. In “in-situ” conditions dirt may appear in the sampler, therefore the 0.5mm gap for each side was necessary to ensure the entry and exit of the liner in the sampler in the start and in the end of the sampling process. The sampler had a useful length of 500mm that makes the expectable frequency of the EMM-ARM test with the PVC liner between 45Hz and 130Hz. The Figure 31 shows the sampler dimensions and Figure 32 the sampler and the detail of the cutting edge:

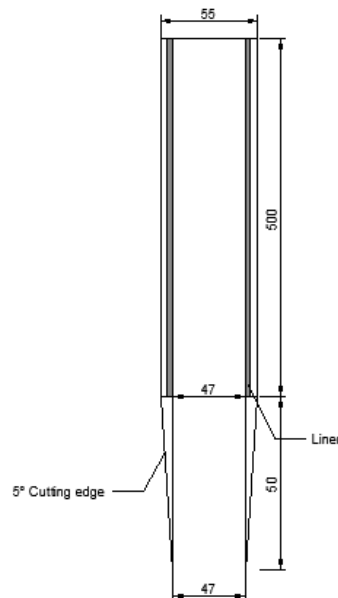


Figure 31 - Dimensions of the sampler (mm)



Figure 32 - Sampler and detail of the cutting edge

The AR of the sampler was 36.9%, a value fairly superior to those proposed by the state of art, which is due to the use of a liner and to the thickness of the sampler. Under the circumstances to have an AR within the recommended limits the sampler should have to have a much bigger diameter that would compromise the manoeuvrability and would considerably increase the material required for the experimental program. To compensate the high AR following the recommendations of the state of art a 5° cutting edge was selected. The sampler with the liner inside had no ICR to maximize the sample quality, the jamming should not be a problem as a load actuator will be used to drive the sampler into the layer. The length of the liner should be as nearly the same as that of the sampler in order to distribute the load of the actuator with the steel of the sampler and to prevent the liner from moving during driving. The thickness of the sampler was supposed to be enough to resist the load.

To test the mechanical of driving a sampler into the soil and to identify potential problems in the final layer it was performed a preliminary test that consisted in a layer of sand inside of a circular container of about 60cm. The sampler was driven into the soil by putting weights on the sampler. The pushing was not continuous, as the weights were put on the sampler when the sampler stopped the movement. The Figure 33 shows the container with the sampler.





Figure 33 - Preliminary test

In this preliminary test the liner had a length larger than the sampler to facilitate the removal of the liner out of the sampler. The experiment allowed some observations:

- The sampler was driven with ease until 20% of the length of the sampler. At such point, the necessary force for driving was very much increased. This might be partially explained by jamming effects due to the lack of an inside clearance before the cutting edge in the sampler;
- To remove the sampler from the soil it was necessary to dig around the sampler for about a fourth of the length of the sampler and then pull the sampler out;
- The sample maintained its consistency after the liner was removed from the sampler but movements, particularly the vertical ones, may disturb the sample thus a careful manoeuvrability of the liner is of utmost importance to keep the sample undisturbed.

For the test of the sampler in the pilot application a load actuator that is in the University of Minho that allows a continuous movement on the sampler will be used. The procedure can be seen in Figure 34, the equipment consists in two concentric tubes in which the smaller tube applies the load on the sampler. Despite the recommendations on the literature about the importance of a single push on the sampler into the soil (Hvorslev 1949) the smaller tube has a length of 30cm thus the sampler will be driven in two stages. A scheme of the driving procedure can be seen in Figure 34.

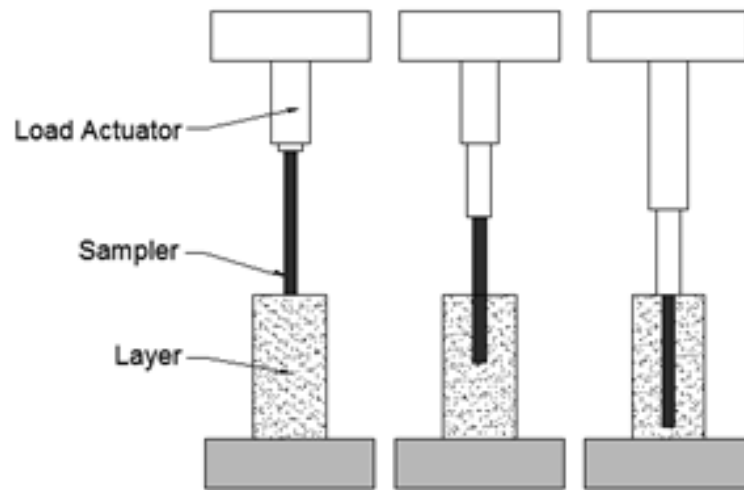


Figure 34 - Driving procedure

In the first stage the sample will be driven until 300mm depth and in the second the remaining 300mm.

## 4 EXPERIMENTAL PROGRAM

The experimental program had the purpose of testing the proposed sampler for EMM-ARM experiments. For that it was necessary to create a pilot layer in order to simulate in-situ conditions. It was required to characterize the mixture of soil-cement particularly the compaction level. After the layer was ready the sampler was driven into the soil and the samples for EMM-ARM testing were retrieved. This chapter presents the utilized materials, the experimental program of the pilot application and the discussion of the corresponding results.

### 4.1 Materials and mixture proportions

#### 4.1.1 Soil

The sand was a uniform river sand composed mainly of quartz that was selected because a similar sand had already been used previous works (Costa 2011; Silva 2010; Magalhães 2013; Silva *et al.* 2013). The sand was sieved to characterize its grain size distribution, following the E 262-1972 (LNEC) standard. The results are presented in Table 5 and in Figure 35.

Table 5 - Grain size of the sand

Sieve Number	Diameter (mm)	Passed(%)	Retained(%)
4	4,76	100,0	0,00
10	2,00	99,2	0,82
20	0,85	96,6	2,57
40	0,425	57,1	39,49
60	0,25	10,8	46,31
80	0,18	4,3	6,46
140	0,105	2,2	2,16
200	0,074	2,1	0,07
	Pan	0	2,11
		Sum	100,00

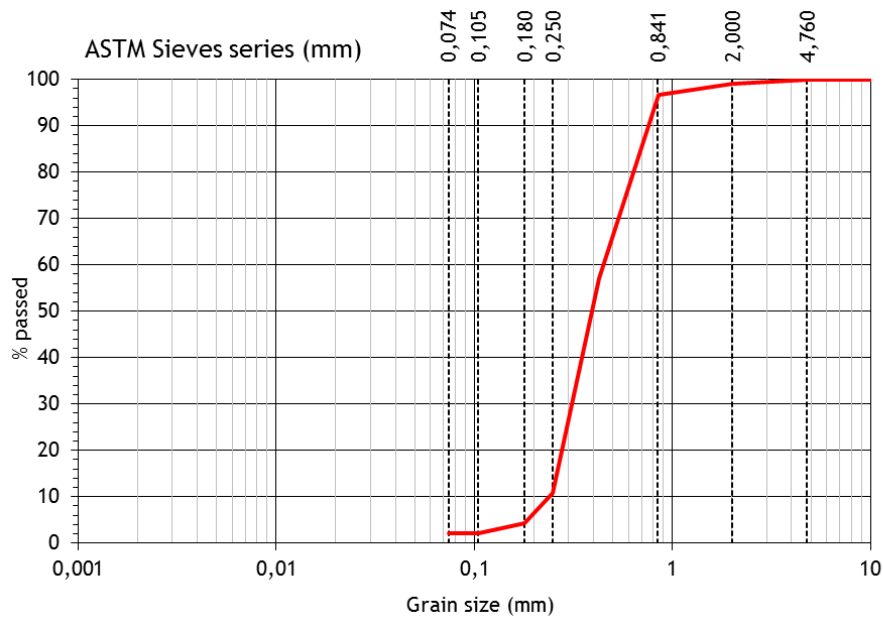


Figure 35 - Granulometric curve of the sand

It was concluded that the sand was relatively monogranular because 85,8% of the grains were retained either in 0,425mm sieve or in 0,25mm.

The standard proctor test following the Portuguese standard E 262-1972 (LNEC, 1972a) was performed for the determination of the maximum density of the sand. The results are presented in the Figure 36. The optimum water content is of about 10% and the sand dry density of 1834 Kg/m<sup>3</sup>.

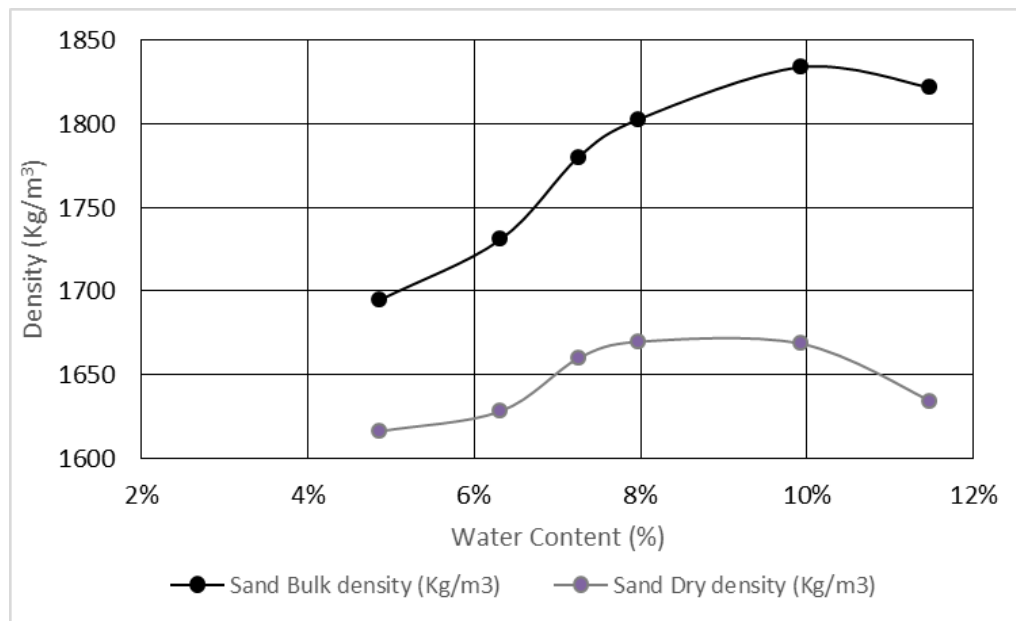


Figure 36 - Compaction curve of the Sand

#### 4.1.2 Cement

The cement used was the CEM II/ B-L 32.5N (supplied by CIMPOR) because its use is very widespread in Portugal, thus being strongly representative. No specific testing was performed to characterize the cement but according to information on a datasheet of the supplier (Datasheet Cimpor 2004) the clinker is between 65% and 79% and the limestone between 21% and 35%. The setting time is above 75 min and the expansion below 10mm. The minimum compressive strength at 7 and 28 days are 16 and 32.5 respectively.

#### 4.1.3 Mixture proportions

The mixture was composed by the sand, 7% of cement and 9% of tap water, all quantities were measured in terms of the dry mass of sand. This mixture was chosen because of its similarity with previous works that comprised application of EMM-ARM to stabilized soils. This mixture has a relatively high content of cement, as to have significant evolutions of E-modulus and thus better illustrate the wide range of applicability of EMM-ARM To determine the maximum density for this mixture the standard proctor test following the Portuguese standard E 262-1972 (LNEC, 1972a) was applied. The results are presented in the Figure 37. For this particular mixture, the optimum water content is of about 9,6% and

the maximum dry density of about  $1976 \text{ Kg/m}^3$ . Nonetheless, for continuity with previous works as mentioned above, 9% of water was selected for the mix.

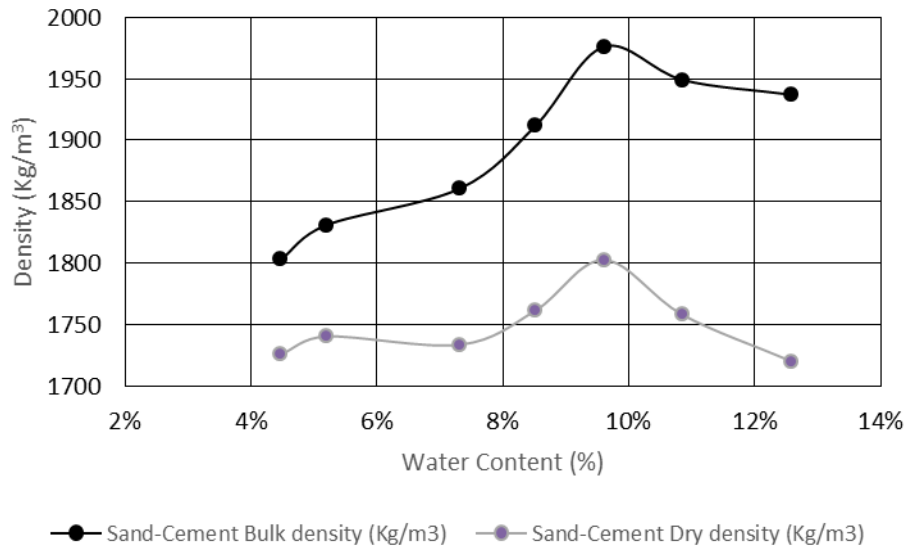


Figure 37 - Compaction curve of the Sand-Cement mixture

## 4.2 Pilot application

### 4.2.1 Overall Strategy

In this preliminary phase of testing it was decided to perform the tests in laboratory environment. The strategy followed in this pilot application is summarized in Figure 38. First it was necessary to create a layer (Figure 38a) that can adequately simulate the in-situ conditions for a representative test of the sampler. In previous works of the research team at the University of Minho, a wooden box with inner dimensions of  $1\text{m} \times 1.5\text{m} \times 0.3\text{m}$  (450 litres) (Silva *et al.* 2014) was used as a container for the layer. As the sampler developed in the scope of this work has 55cm of length, and is aimed to be inserted from the top surface of the stabilized soil, the layer would need to have a minimum height of 60 cm to allow full insertion of the sampler and obtaining a complete sample. Due to the lack of human and mechanical resources for the creation of a layer with the same plan dimensions as the previous work, it was decided to perform the sampling (Figure 38b) on a simulated layers with much less volume, and thus much more practical in terms of logistics and cost. For such purpose, the layer from which the samples were gathered was materialized by placing the freshly stabilized soil into a 35cm diameter tube, with 70cm height. The tube was a commercial formwork made of multi-laminated paper layers, which

was considered robust enough for the placement of stabilized soil and enduring the mechanical disturbance associated to the insertion of the sampler in the stabilized soil. The diameter of 35cm was chosen as to ensure a reasonable distance between the external walls of the sampler and the inner walls of the tube into which the soil was placed as shown in Figure 40. To have the possibility of comparing results two layers were performed.

To corroborate the results of the sampling three reconstituted specimens, for unconfined cyclic compression (UCC) tests were carried out (Figure 38c) For both tests the aimed bulk density of the mixture was  $1970 \text{ Kg/m}^3$  (same as the one targeted in the layers made in the tubes). Each UCC was performed at the age 10 and 29 days.

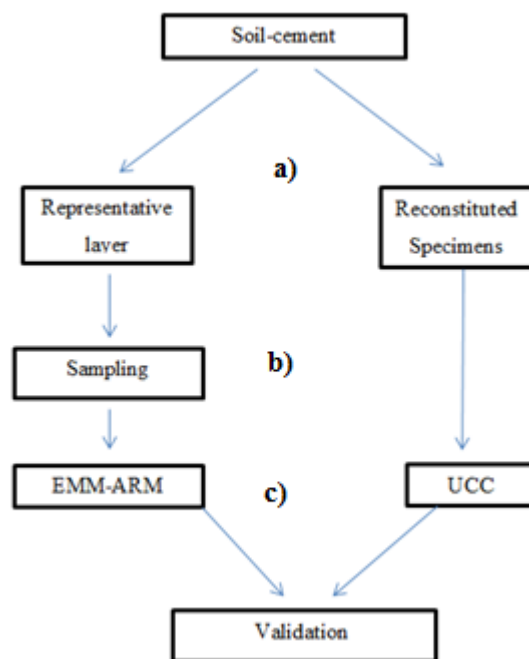


Figure 38 - Overall Strategy

#### 4.2.2 Preparation of the mixture and placement

For each tube it was necessary to mix 114.7kg of sand 8kg of cement and 10.3kg of water for a mixture composed by 9% of water and 7% of cement, measured in terms of the dry mass of sand. The internal volume of each tube was 67 litres, whereas the mixer had a maximum capacity of 50 L. Therefore, two consecutive batches were necessary for each tube. The sand was placed inside of the mixer bucket, the mixer was turned and the cement was added. After the cement was placed into the bucket the mixer operated for more 5 minutes. After that the water was added and the mixer operated continuously for more 5

minutes. The instant  $t=0$  for the tests is considered the time at which the water was mixed with the sand-cement in the first batch.

After the conclusion of the first batch the mixed material was compacted while another batch was prepared. The compaction was performed inside of the formwork tube in five parts of 14cm each through a jack hammer (model Kango type 638). The bulk density was controlled by the amount of material for each part.

The specimens for the UCC tests were reconstituted in a metallic mould with 200mm height and an inside diameter of 100mm. To ease the disassembling of the mould a membrane of Polytetrafluoroethylene commonly known as Teflon was used.

The compaction of the specimens were made in 3 stages of 66,6 mm and started after the preparation of the mixture. The quantity of material necessary for each stage was measured and then placed in the mould as can be seen in Figure 39 a. The compaction started with the use of a wooden pestle (b) and ended with the use of a mechanical jack (c) to ensure the necessary height of the layer.

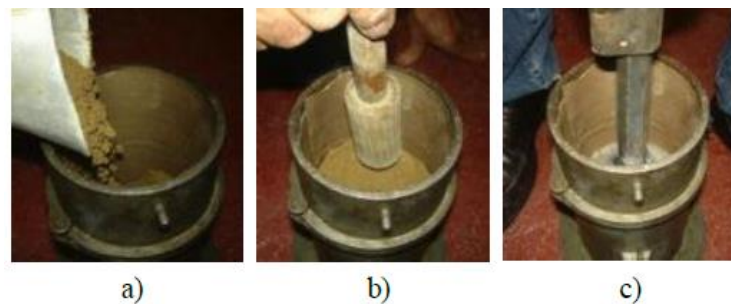


Figure 39 - Preparation of the UCC Specimen adapted from (Magalhães 2013)

### 4.2.3 Sampling

The sampling was performed immediately after the final compaction of each tube, as to allow EMM-ARM results in the earliest ages possible. The procedure started by manually guiding the sampler on layer, centred with the formwork tube to ensure that the sampler was driven without deviating and to centre the sampler to the load actuator. As mentioned above the sampler was driven in 2 stages of 30 cm. The apparatus is presented in Figure



40. The load applied by the load actuator on the sampler in both collecting trials was recorded.

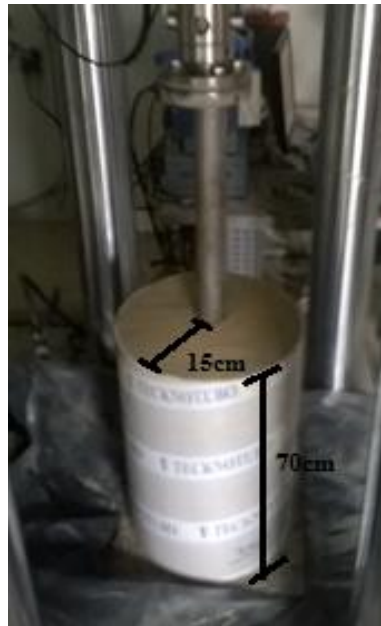


Figure 40 - Apparatus of the sampling

After driving the sampler it was necessary to remove the soil around the sampler until the sampler could be easily removed from the tube. The next step was to remove the liner from the sampler that was completed by slowly tilting the sampler until the liner started to slide through the sampler. On each side of the liner 25mm of material was removed with a spatula to apply the wooden disks and the screws for the supports, the beam had then 500mm of length.

#### 4.2.4 Description of the test procedures for E evaluation

After sampling, the beam was placed under simply supported conditions, the accelerometer was attached to the beam and the monitoring was started. Figure 41 shows the apparatus.

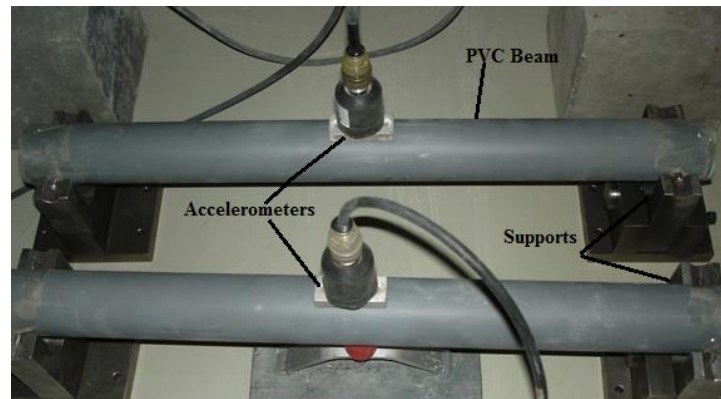


Figure 41 - EMM-ARM test

To measure the accelerations piezoelectric accelerometers (PCB) were used, as shown in Figure 42a. The accelerometers had a sensitivity of 10V/g, a frequency range of 0.15Hz-1000Hz and a weight of 210g. The data of the accelerometer were measured through a signal acquisition system (National Instruments 24-bit NI-USB-9234 with 4 channels), presented in Figure 42b, connected to a computer with a Labview code designed for the EMM-ARM test. The test started at  $t=4h$  for both EMM-ARM beams and monitored the first 28 days of hardening.



a)



b)

Figure 42 - a) accelerometer b) signal acquisition system (Costa 2011)

The procedures for the UCC tests followed the same approach as reported in previous works of the applications of EMM-ARM to stabilized (Silva 2010; Magalhães 2013; Silva *et al.* 2013).

The UCC tests were performed with load application through a 50 kN hydraulic actuator, which included a load cell. The strains were measured on-sample through three transducers (LVDTs) that were supported by two rings screwed to the specimens. Figure 43 presents the apparatus for UCC testing.



Figure 43 - UCC setup

The range of the strains for the tests followed the previous works of Gomes Correia *et al.* (2006) and Gomes Correia (2004) according to which the amplitude of the loading-unloading cycles should be small enough to ensure that the strain response cycles are closed and nearly linear, thus strains should be kept within  $10^{-4}$ . The UCC tests were performed at distinct ages so the maximum stress was adjusted to be about 10% of the ultimate strength at the age of testing of which the value was obtained from previous works that used the same mixture (Silva 2010). The tests consisted of three continuous loading-unloading cycles and started with a pre-load of 300N which increased, at a 50N/s load rate, until the maximum strain at the age of testing was achieved.

#### 4.2.5 Results

The load applied by the load actuator and the displacement of the sampler recorded during both trials of the sample collection are presented on Figure 44. The figure allows the

observation that a significant force was necessary to drive the sampler, reaching a maximum final value of 32 kN. Possibly, that could have been avoided if the ICR index of the sampler were larger than 0. Such ICR would have allowed some expansion of the material in the entrance of the liner. That would have reduced the amount of load necessary but could have compromised the sample quality as it would possibly reduce the bulk density of the specimen (Marcuson III & Franklin 1979).

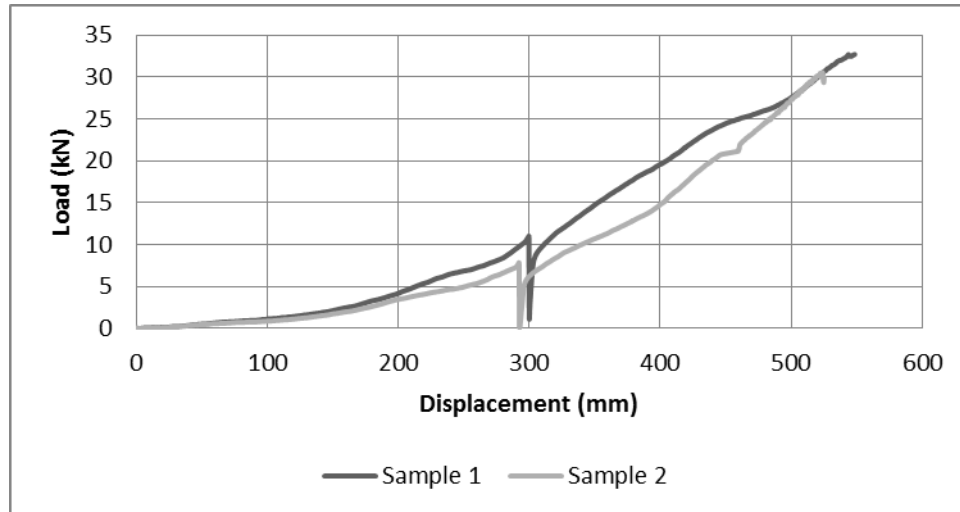


Figure 44 - Load-Displacement curve for the sampler

As a comparison of the magnitude of the load, the force required for driving a similar sampler ( U100) into red clays (Hallam & Northmore 1993) is of about 14kN which is half of the value of the EMM-ARM sampler for the sand-cement.

After sampling each mould with the material, it was weighted and, after compensation of the weight of the PVC tube, the bulk density for sample 1 was  $1994,41 \text{ kg/m}^3$  whereas for sample 2, the bulk density was  $1969,32 \text{ kg/m}^3$ . The slight difference between the two samples may be partially explained by some deviation on entry of sampler into the layer. As a matter of fact, such situation is corroborated by the overall higher load that was necessary to drive the sampler into layer 1 (as compared to layer 2). Both samples were representative of the conditions of the layer as it was compacted for a target bulk density of  $1970 \text{ kg/m}^3$ .

Figure 45 shows the results of the frequency evolution along the curing time for both EMM-ARM samples. The results were very similar for both samples and varied from 50Hz to 122Hz.

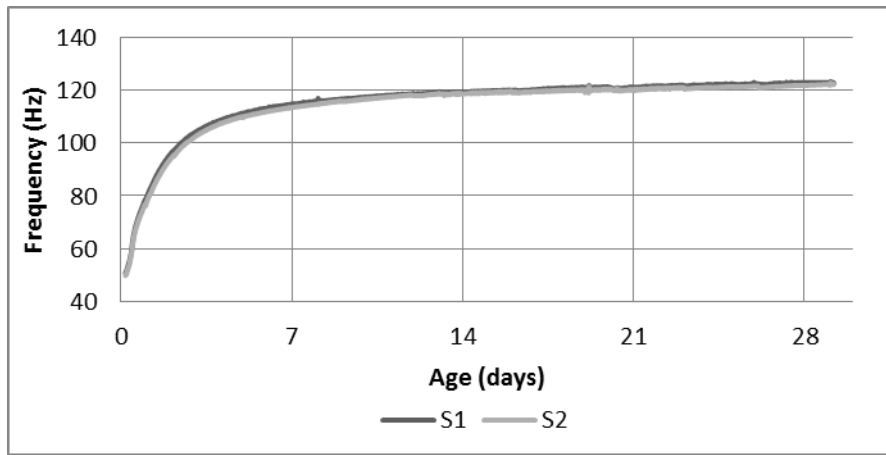


Figure 45 - EMM-ARM results

In regard to data collected from UCC testing, an example of the experiment made at the age of 10 days is shown in Figure 46. A very good linearity of response can be observed, with a  $r^2$  coefficient of 0,95.

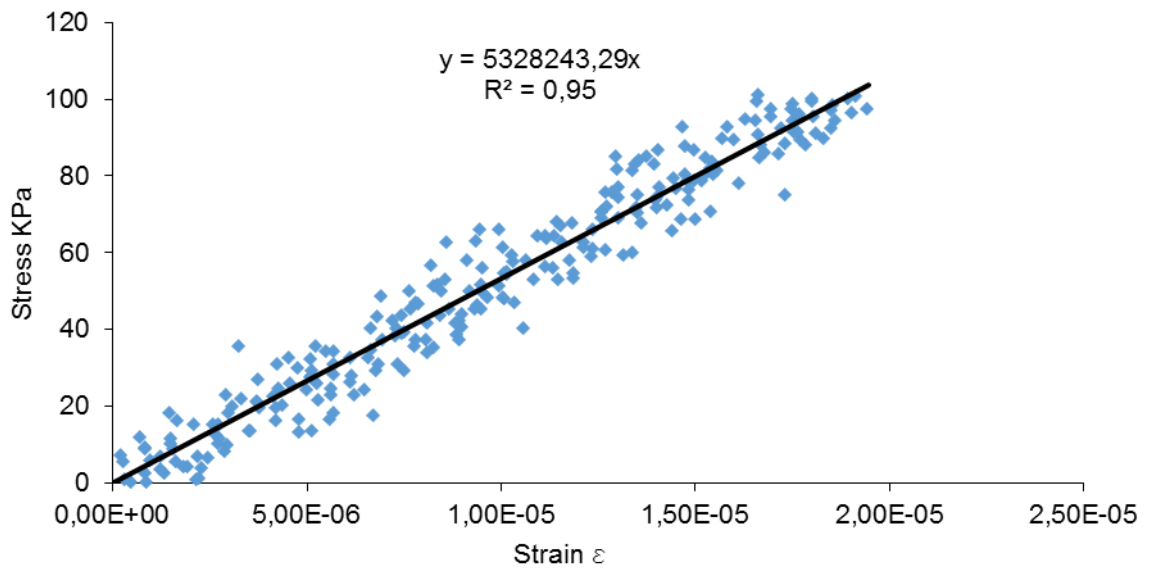


Figure 46 - UCC stress-strain relationship

The Table 6 shows the results for each UCC specimen.

Table 6 - UCC specimens results

Specimen	Bulk density (Kg/m <sup>3</sup> )	Results at 10 <sup>th</sup> day(GPa)	Results at 29 <sup>th</sup> day (GPa)
UCC1	1981	5,68	7,23
UCC2	1960	5,33	6,29
UCC3	1972	5,91	6,31

The E-modulus values computed from the resonant frequencies of the two specimens are presented together with the UCC test results in Figure 47.

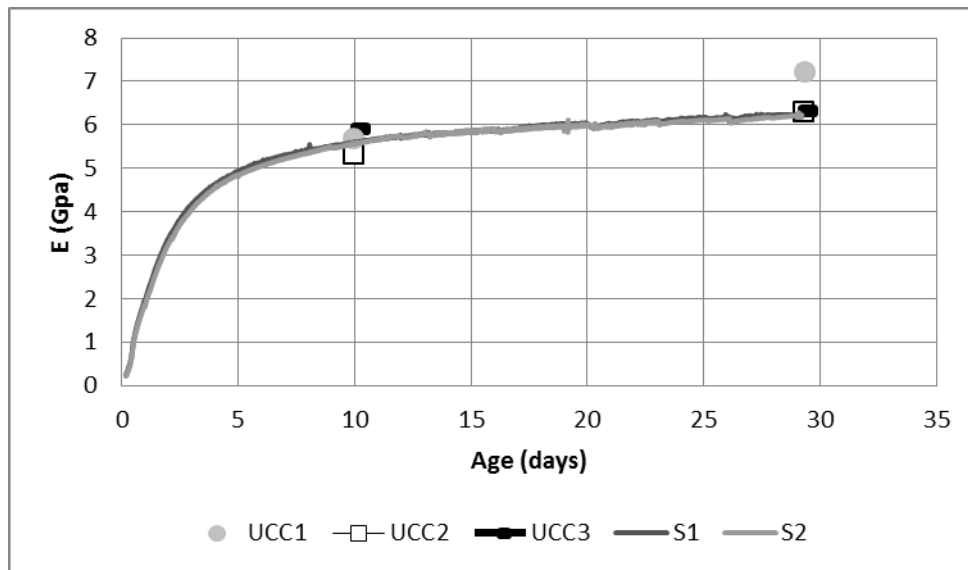


Figure 47 - EMM-ARM vs UCC test results

The results of the EMM-ARM tests were validated by remarkable coincidence with the available UCC results. On the 10<sup>th</sup> day of hardening the results of EMM-ARM (about 5.6 GPa) were within the UCC tests ( between 5.3 and 5.9 GPa). On the 29<sup>th</sup> day the first UCC test presented a significant difference to EMM-ARM (1GPa) but the other two tests practically matched the EMM-ARM (0,1 GPa of difference).

The coherence of the results of the samples retrieved from the layer with the UCC results, aligned with previous works (Silva *et al.* 2014; Silva 2010), indicates the feasibility of the sampling technique used in this dissertation. Thus the EMM-ARM methodology now has a sampling process that allows the retrieving of samples that represent “in-situ” conditions. However, the sampling process still needs more tests with other mixtures and conditions to improve its robustness to face real situations.

## 5 PROPOSAL OF A VARIANT OF EMM-ARM

### 5.1 Concept

Applying the EMM-ARM technique to stabilized soils demands a relatively intricate preparation of the experimental setup, particularly in regarding to the sampling procedure. Bearing such aspect in mind, a variant to EMM-ARM has been studied in the scope of this dissertation, with two main aims (i) avoiding the necessity of complex sample collection and the inherent uncertainties regarding the representativeness of the soil; (ii) having a methodology that allows direct testing of the stabilized layer as to obtain its corresponding E-modulus. The technique to be adopted is schematically represented in Figure 48 and consists in partially embedding a slender steel plate into the stabilized soil, and continuously monitoring its resonant frequency at the free edge. The variation of the stiffness of the stabilized soil into which the steel plate is embedded changes the extent of clamping/fixing, thus inducing variations in the resonant frequency of the plate. It is then possible to infer the stiffness of the stabilized soil based on the variations of resonant frequency of the steel plate. The pioneering application of this technique to concrete, also conducted at the University of Minho by the PhD student José Granja, has conducted to very promising results, particularly for assessing stiffness values below  $\sim 1\text{GPa}$  (Azenha *et al.* 2012).

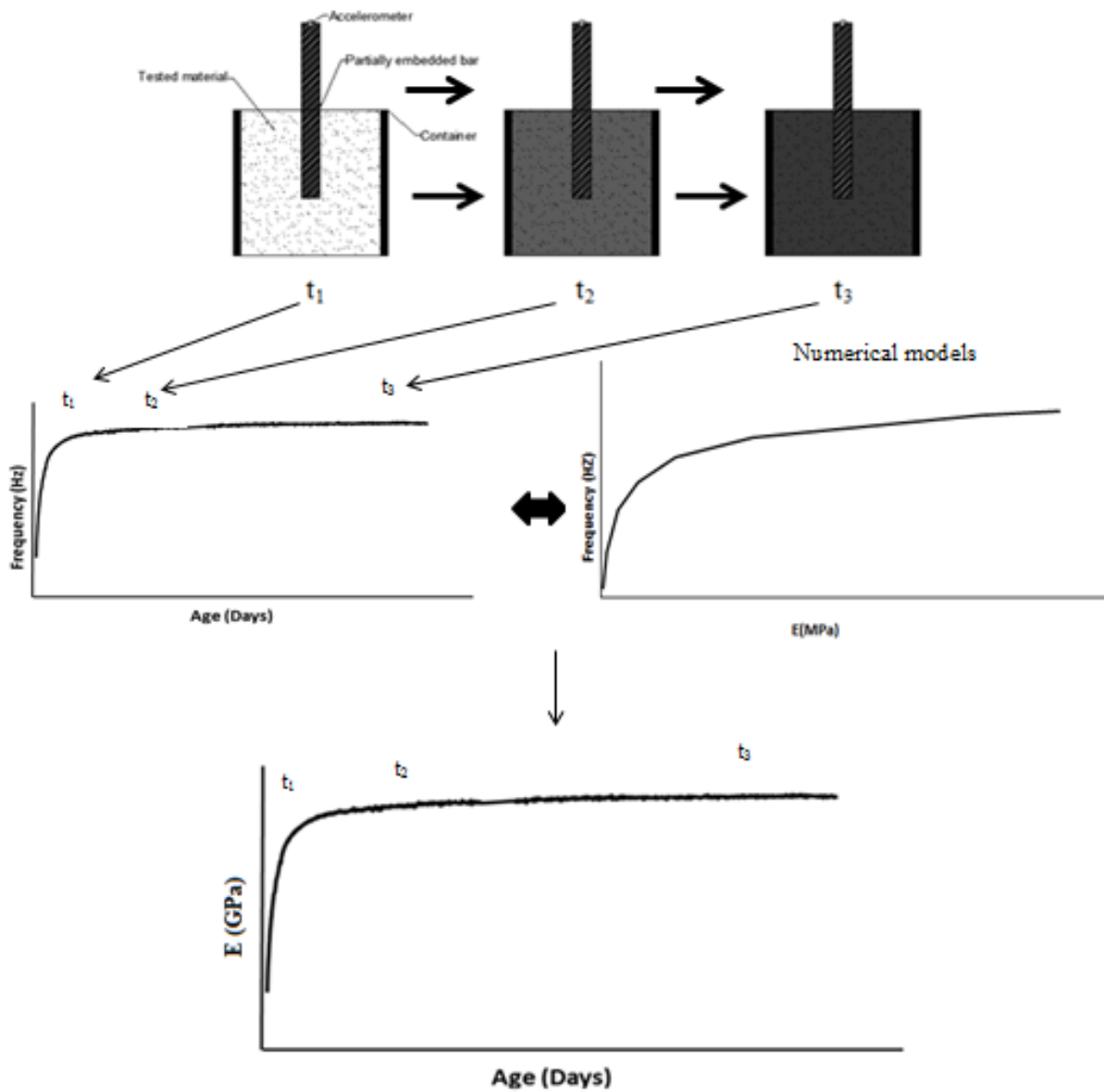


Figure 48 - Scheme of the concept

A literature review related to the proposed methodology led to the knowledge that a similar technique using this concept had already been applied to another hardening material: resin based materials in the context of dental science (Meredith 1999). Such technique includes the determination of the elastic modulus of resin based materials during polymerisation as function of resonance frequency of a beam inserted into the tested material. In this technique, represented in Figure 49, a transducer composed by an L-shaped titanium beam to which two piezo-ceramic elements were attached, was vibrated by exciting one of the piezo-ceramic elements with a sinusoidal signal. The other piezo-ceramic measured the response. The transducer was mounted at its base in a small specimen of the material to test and behave as a cantilever beam. After the setup is mounted it was possible to observe



the evolution of the resonance frequency of the beam during the curing time. At such research work, the authors were not able to relate the resonance frequency with the elastic modulus directly. It was suggested that for future works the value of the resonance frequency could be related with values of elastic modulus determined by standard quasi-static test methods.

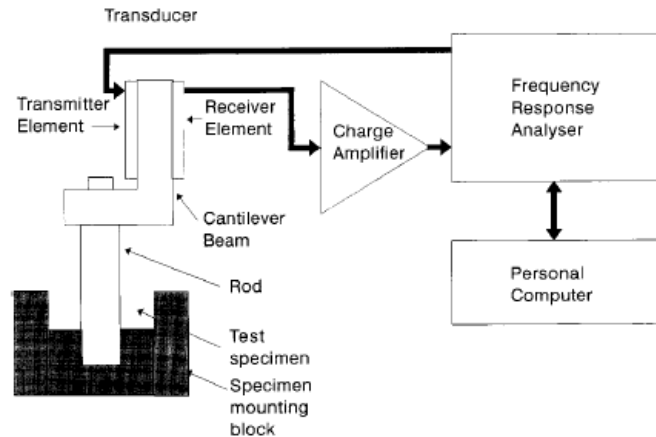


Figure 49 - Schematic showing transducer and specimen well connected to charge amplifier, frequency response analyser and personal computer (Meredith 1999)

In spite of the relatively similar previous attempt to resins, the variant to EMM-ARM proposed above has originalities and potential that made it worth testing in the scope of stabilized soils. There are however added challenges in regard to the conversion of resonant frequency values into estimated  $E$ -modulus values of the tested materials through an analytical formulation. Instead, the present research work focused on using numerical models that simulate the experiment as to obtain the relationship between  $E$  and  $f$ .

## 5.2 Proposed pilot model

### 5.2.1 Performance requirements

In view of the general principle of a cantilever that is partially embedded in the stabilized soil to be tested, the following performance requirements were set for its first trials:

- The embedded beam should be slender enough as to be easily excitable and facilitate modal identification processes;

- The beam should not have similar resonant frequencies in each bending direction, thus non-circular and non-square cross sections are desirable to ensure that the direction of the 1<sup>st</sup> resonant frequency is clear (e.g. rectangular cross-section);
- The variation of the resonance frequencies during the test needs to be maximized for a better identification of the elasticity modulus;
- The resonance frequency of the global system (container + tested material + beam) should have little interference with the vibration of the local system (beam) thus the global system should be much stiffer than the local system.

### 5.2.2 Preliminary numerical studies

The dimensions/geometry of the model studied in this dissertation was selected considering the existing commercial materials and a study made at the University of Minho by the PhD student Jacinto Silva (yet unpublished). Such study involved several parametric analyses regarding the importance of each variable of the problem. The main conclusions of such study are summarized below:

- The system is very sensitive to small changes in the length of the cantilever;
- The embedment length does not have a significant effect on the resonant frequency of the beam. The first ~5 cm have the most influence, though;
- Increasing the slenderness of the beam (higher span and smaller cross-sectional dimensions) allows a better excitability. However, very slender beams lead to loss of sensitivity of the beam resonance in regard to the material that ensures its fixed extremity (i.e., the tested material);
- The shape of the container into which the tested material is placed (in the context of laboratory applications may be as small as 0,25 x 0,25 x 0,25 m<sup>3</sup>) does not have significant interference on the results when considering a reasonable distance from the beam to the borders of the container;
- As the stiffness of the tested material increases, the corresponding frequency variation of the embedded beam decreases significantly and non-linearly. This is caused by the approximation to the conditions of a perfectly fixed support, thus converging to an asymptotic maximum resonance frequency.

Such mentioned work by Jacinto Silva led to the conclusion that a good compromise among the aforementioned observations could be assured by using a rectangular steel beam with 30mm×4mm cross-section, with a total length of 300mm (150mm of which embedded

into the tested material). A circular container with 250mm diameter and 250mm length was considered enough to avoid the disturbance of wall effects. The proposed model is presented in Figure 50 and included a 25-gram accelerometer with its centre fixed at the top of the bar and a wooden base connected to the PVC tube.

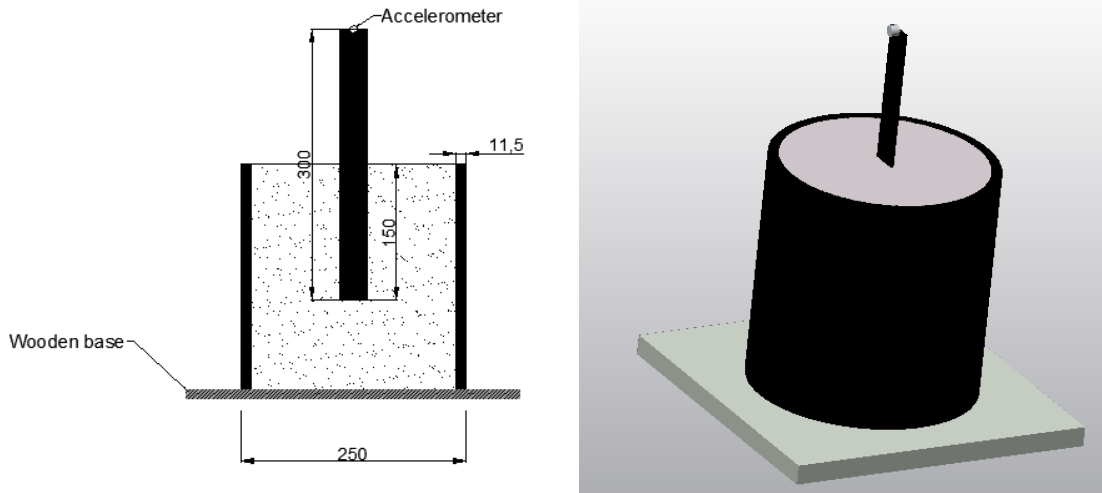


Figure 50 - Sketch of the proposed model (dimensions in mm) and 3d view from Multiphysics

### 5.2.3 Detailed simulations of the proposed setup

In order to obtain the relationship between the resonant frequency of the beam and the E-modulus of the tested material, several numerical simulations were made in the scope of this dissertation. The proposed model was simulated though Autodesk Simulation Multiphysics 2013 in order to obtain the expectable resonant frequency as a function of the E-modulus of the stabilized soil.

The simulation model was composed by the wooden base fixed to the PVC tube, the embedded bar and the treated soil. The accelerometer was simulated by a mass on the top of the bar. For the supporting conditions was considered that the lower surface of the wooden base had all its nodes fixed to the ground.

The mesh of the FE model can be seen in Figure 51 (total of 4252 elements). Each part of the model was modelled as a brick element, the material was considered isotropic and it was used the 2<sup>nd</sup> order integration.

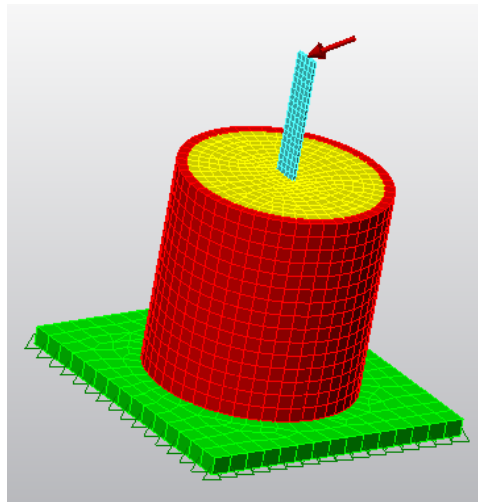


Figure 51 - Numerical model

The mechanical properties of the steel bars to be used in testing were determined in the laboratory, with the same hydraulic actuator mentioned in Chapter 4 and under displacement control (2mm/min). Two steel bars were tested, and the values of 203GPa and 210GPa were obtained for each bar. In the simulation model, the average value of 205GPa was considered for the steel bars.

For the tested stabilized soil, E-modulus was varied within the range of expectable values, between 50MPa and 6000MPa. The stiffness values of PVC and wood were obtained from the library of the calculation software: 2,75GPa for the PVC and 9GPa for the wood. No special accuracy was required for PVC and wood, as their behaviour has negligible effects on the resonant frequency of the tested bar (according to the preliminary parametric analyses. The Poisson's ratio also an insignificant effect on the results, thus were used standard values from the software.

After the simulation, for each of the expected values of elasticity modulus the resonance frequency was registered, the corresponding graph is shown in Figure 52. These values will be used to relate the frequencies of the experimental model with the elasticity modulus.

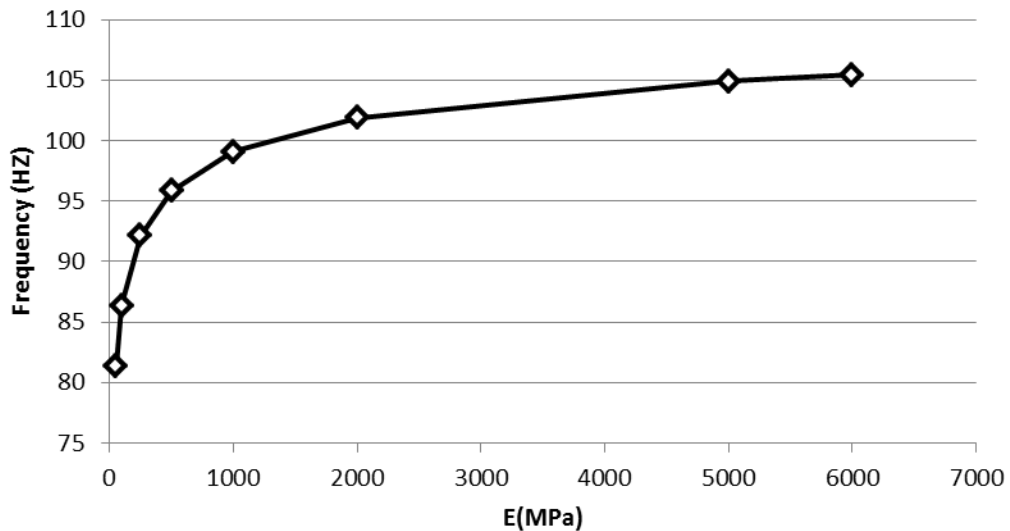


Figure 52 - Computed relationship between the resonant frequency of the embedded steel bar and the E-modulus of the tested material

As can be seen in Figure 52 the model has a good resolution for lower values of E meaning that until there a small variation of the elasticity modulus signifies a large variation of frequencies. For higher values of E the model is very sensitive to the frequency as small variation of the frequency signifies a large variation of E.

The resolution of the model can be better revealed by the derivation of the frequency with the respect to the modulus. The derivative is presented in Figure 53.

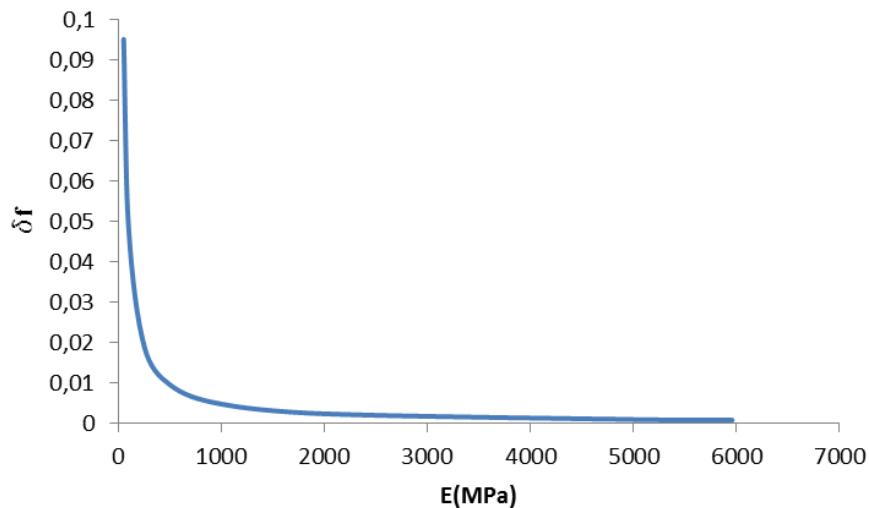


Figure 53 - Derivative of the frequency

As can be observed the resolution is remarkable until about 500MPa when starts to degrade. At higher values the resolution tends to zero. In practical terms this degradation is

explained by the tendency of the beam to starts to behave as a perfectly fixed support instead of an embedded beam.

It was verified through the numerical analysis that the first mode has low interference from other modes. The computed three first modes are presented in Table 7.

Table 7 - The three first modes

E-soil(MPa)	Mode	Frequency (Hz)
50	1	81,41
	2	185,622
	3	191,34
5000	1	104,93
	2	533,535
	3	555,72

The second and third modes of resonance frequency have very different values in relation to the 1<sup>st</sup> mode hence they should have low interference on the test.

The difference between the modes increases with the increase of the elasticity modulus of the stabilized soil because the second and third modes are global modes of the system that is essentially controlled by the tested material instead of the bar as can be observed in the software.

### 5.3 Pilot experiments

#### 5.3.1 Experimental setup

The construction of the model started by the preparation of the necessary parts and materials. The steel bar of 30mm × 4mm was bevelled as presented in Figure 54, in order to ease the driving into the stabilized soil.



Figure 54 - Beam used and sharpened edge

The container used for the layer was a 250mm PVC-tube, as presented in Figure 55 that was glued to a wooden plank to ease the transportation and to prevent soil losses.



Figure 55 - PVC container

### 5.3.2 Strategy and procedures

A pilot experiment of the variant to EMM-ARM was performed, with three equal specimens being simultaneously assessed through this new experimental technique. It was intended to perform a comparison with the results obtained for the same stabilized soil in

previous EMM-ARM tests (already presented in Chapter 4). Thereby the target bulk density of the material inside the container was the same as in the layers of the chapter 4.

The mixture of the soil-cement used was prepared and comprised by the same materials of the previous chapter. Hence the mixture was composed by 7% of cement and 9% of water and a aimed bulk density of  $1970\text{Kg/m}^3$ .

The compaction was performed inside of the PVC container in three parts of 8,3 cm each through a wooden pestle as can be seen in Figure 56a. The bulk density was controlled by the quantity of the material for each part. After the compaction the container was involved on the top with a plastic sheet (Figure 56b) to prevent water losses.

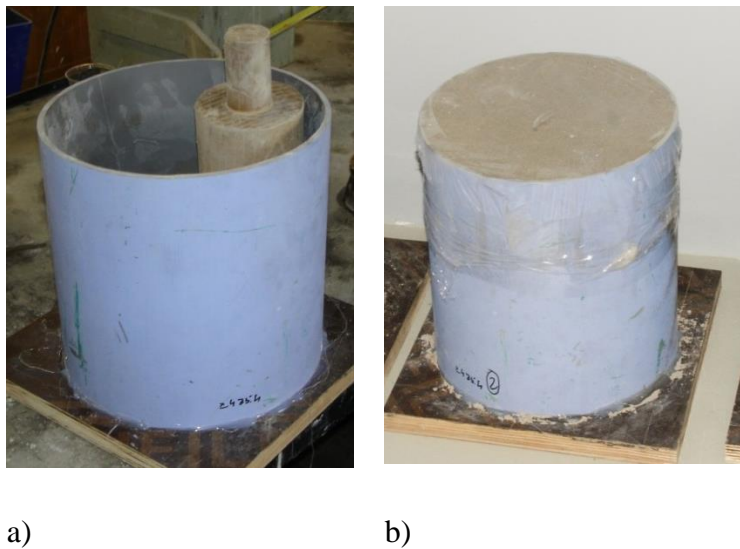


Figure 56 - a) PVC tube with the wooden pestle b) Plastic sheet involving the container

Immediately after the end of compaction and plastic sheet protection, the bar was then driven into the layer. This could be initially done by hand-pushing, but after about 10cm of penetration, it was necessary to exert more force for penetration and hammering was necessary. To ensure that the bar was vertically driven a metallic guide supported on the layer and container was used as presented in Figure 57 and Figure 58. The plastic sheet had a previously made slot to allow the penetration of the bar but guaranteeing the correctly hardening of the soil material and no connection to the bar.



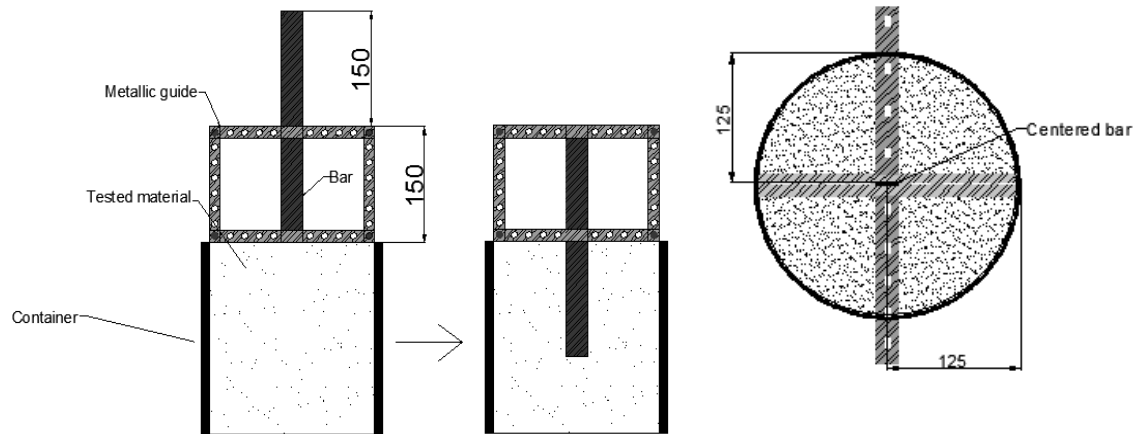


Figure 57 - Scheme of the guide (dimension in mm)



Figure 58 - Beam with the guide

For the measurement of accelerations, a piezoelectric accelerometer (PCB) was attached with its centre at the top of the bar, and connected to a signal acquisition system and a computer. The accelerometers had a sensitivity of 100 mV/g, a frequency range of 0.15Hz-1000Hz and a weight of 25g. The data of the accelerometer were measured through a signal acquisition system (Nacional Instruments 24-bit NI-USB-9234 with 4 channels). The measurement was made for sets of 300s acquired at intervals of 900s. The data were store through the first 15 days. The setup of the experiment can be seen in Figure 59.

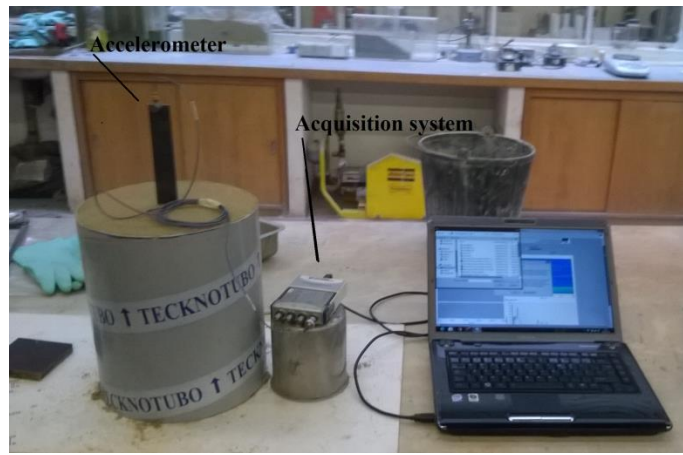


Figure 59 - Setup in a preliminary test

### 5.3.3 Results

The identified 1<sup>st</sup> resonant frequency evolution for each bar (B1, B2 and B3) is presented in Figure 60.

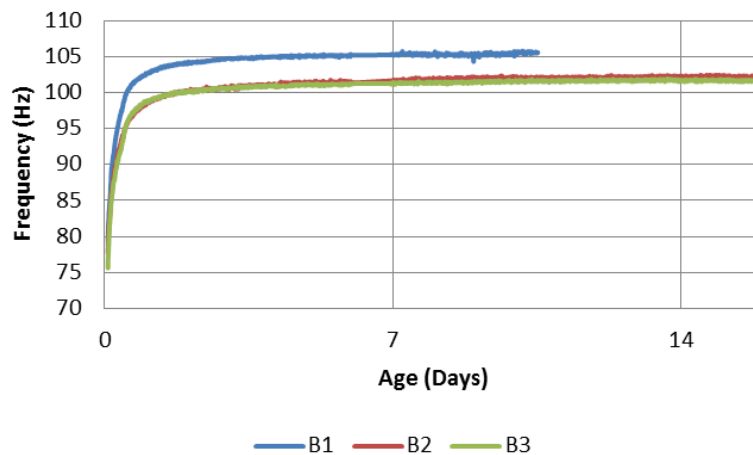


Figure 60 - Results in frequency domain

As can be seen in Figure 60 bars B2 and B3 showed very similar resonant frequencies throughout the entire period of testing. B1 presented higher frequencies during the entire period. It is however clear that the methodology could capture the influence of E-modulus increase in the stabilized soils on the resonant frequency of the bars.

The next step was to convert the data from the frequency domain to an E curve. That was achieved through the correlation of the numerical model results with the frequencies of the experimental model, through the relationship shown in Figure 52. The results are compared

to the EMM-ARM (S1, S2) and UCC tests (UCC1 to UCC3) of the previous chapter. Figure 61 shows the results.

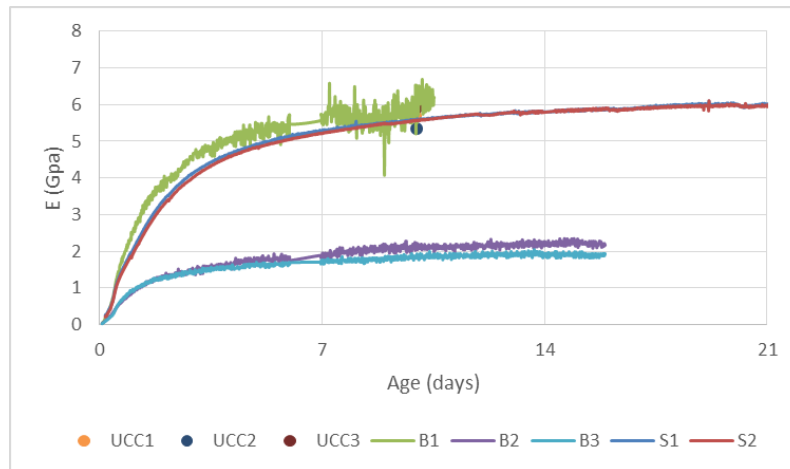


Figure 61 - Results of the new technique compared with the results of the previous chapter. For B1, the results of the new method presented a good agreement with the EMM-ARM and UCC results. However, B2 and B3 exhibited drastic deviations in regard to the EMM-ARM/UCC. The sensitivity of the resonant frequency of the beam to its actual free length and E-modulus, it was decided to perform some sensitivity analyses as detailed in the upcoming sub-section.

### 5.3.4 Evaluation in view of numerical simulations

In order to attempt to recognize possible reasons for the differences in the results between the methodologies a parametric study for each beam was made in the numerical model through the variation of the elasticity modulus of the beam and the length of the cantilever.

For the B1 despite the good results a comparison was made varying the elasticity modulus from the value used in the initial calculations (205GPa) and the maximum value obtained in the experiments of characterization of the steel (210GPa). Figure 62 presents the results for both elasticity modulus as well as the EMM-ARM results.

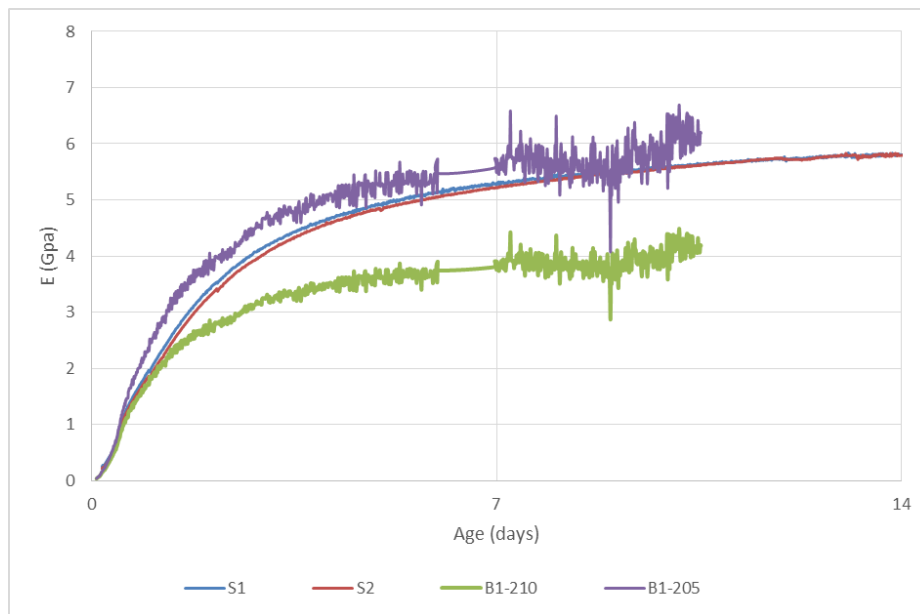


Figure 62 - Results of B1 with an elasticity modulus of 205 GPa and 210 GPa

As can be seen in the figure it is possible to infer that slight variations in the E-modulus of steel can induce very large deviations in the predicted E-modulus of the stabilized soil through the proposed testing technique.

Bars B2 and B3 presented similar resonance frequencies over the monitoring time thus they were approached in the same way. For both bars, a parametric analysis was performed by varying the cantilever length in order to obtain a range of values in which containing within the EMM-ARM results. The length was then varied to 15,3cm and 15,4 cm. The results can be seen in Figure 63 and Figure 64.

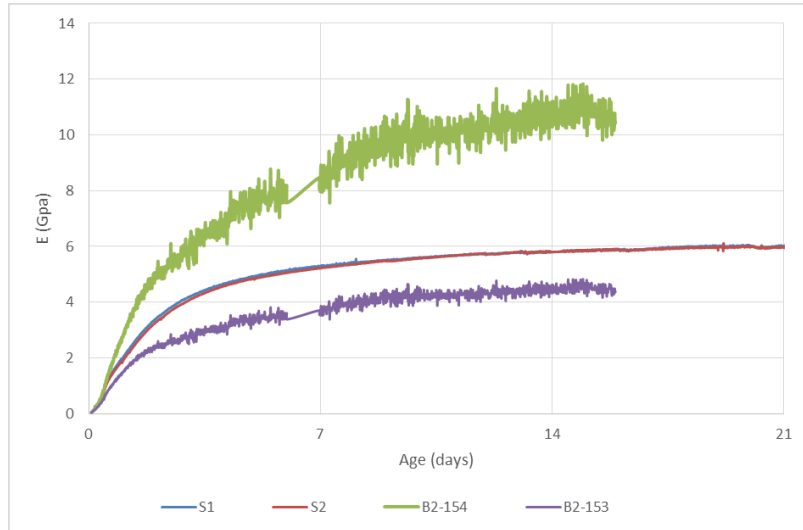


Figure 63 - Results of the bar 2 for a 15,3-15,4cm length of the cantilever

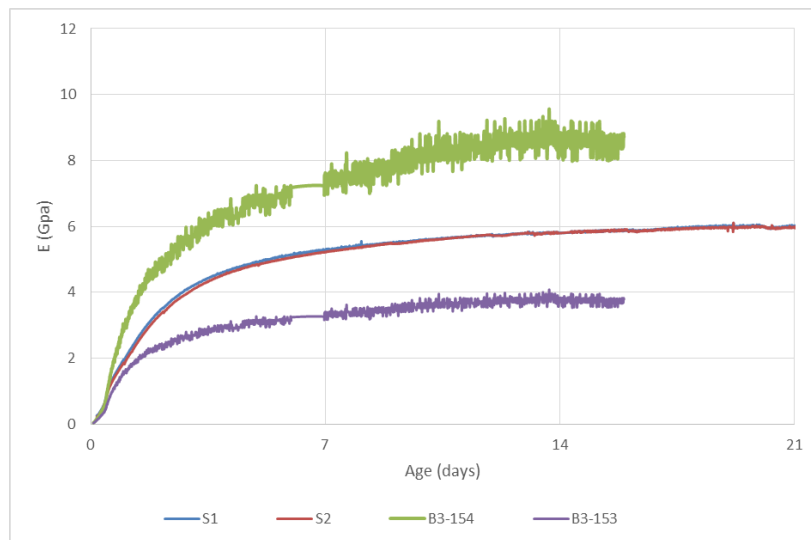


Figure 64 - Results of the bar 3 for a 15,3-15,4cm length of the cantilever

For both bars the correct results could have been achieved with a length of the cantilever between 15,3cm and 15,4cm.

The variability of the cantilever length was very high and its plausibility can be questioned but without more tests to cross results it is difficult to draw more specific conclusions. For these parametric studies were not considered simultaneously variations of the E and cantilever length because it would not have lowered the value of the cantilever.

As can be observed in the results there is little doubt that the technique has potential to become a technique used for the measurement of the elasticity modulus in treated soils.

However this type of analysis on this type of model highlights the importance of the precision of the experimental setup and adequate knowledge of the mechanical properties of the steel bar that is actually under use. The parametric studies performed with this model showed that there are parameters that should be careful controlled for the accuracy of the results namely:

- The elasticity modulus of the bar needs to be identified with a higher level of precision to reduce evitable uncertain of the results;
- The length of the cantilever should be analysed after driving because it is a parameter highly influential on the results;
- This model is more efficient to low values of E because the influence of the tested material on the resonance frequency decreases with the increase of E of the tested material. Thereby the mixture of the treated soil should be modified to appoint for lower values of elasticity modulus in this initially phase of the development of this technique.

## 6 Conclusion

### 6.1 General conclusions

This dissertation was primarily focused on extending the functionality of EMM-ARM, in view of the previous developments at the University of Minho (Silva 2010; Costa 2011; Magalhães 2013; Silva et al. 2013; Silva et al. 2014). Despite the robustness of technique gained with the previous works, it still lacked a sampling method that can be used on in-situ conditions. This dissertation had the purpose of developing the procedure to face practical situations.

For that a sampler that can carry a liner inside while it is driven into the stabilized soil was developed. After retrieving the sample, the liner can be removed and used for the EMM-ARM test. To test if the sampler allowed the recovering of representative samples an experimental program was carried out. The experimental program included two layers and three specimens used for uniaxial compression tests to validate the results.

The feasibility of EMM-ARM results from sampled specimens has been confirmed by the similarity with uniaxial compression tests results. Moreover the retrieved specimens were had bulk density values that were quite similar to those of the layers from where they were collected. Based on the aforementioned observations, it can be said that the EMM-ARM technique can be robustly applied with the developed sampling procedure that allows the retrieving of undisturbed samples.

Despite the portability of the mould that allows deploying the EMM-ARM technique for in-situ quality control, with experiments being conducted at the site laboratory, this technique still has the drawback of requiring sampling, and not measuring the stiffness directed on the stabilized soil layer. Hence, to overcome such issue, this dissertation includes the proposal of a variant of the EMM-ARM technique in which a steel bar of known properties is partially embedded in the layer to be tested. This new variant avoids the necessity of the sampling procedure and the inherent uncertainties regarding the representativeness of the stabilized soil besides being a less time-consuming methodology. This new method involves the modal identification of the resonance frequency of the partially embedded bar, which can be related to the stiffness of the material into which it is embedded.

An experimental program with three layers was performed for the development of this new variant and the respective modelling of the model was performed. The performed layers intended to have the same soil-cement characteristics of the previous experimental program to have the possibility of comparing results. Even though the results were rather good in one of the three tested steel bars (quite similar to EMM-ARM), the other two led to rough underestimations of the stiffness of the stabilized soil. A parametric numerical analysis has revealed that this new methodology for E-modulus estimation is quite dependent on small deviations in the cantilever length or material properties, thus demanding very high levels of control and measurement.

This new methodology seems to have potential to become used on in-situ conditions but it still is at initial stages of development, thus requiring further detailed studies and improvements.

## 6.2 Future Developments

The EMM-ARM technique has a robustness that allows it to be used in most of the situations for which it was targeted. However, a few potential enhancements can still be done such as:

- The sampler should be tested with a liner of smaller length in order to allow the retrieving of samples in stabilized layers of small thickness (e.g. 40cm);
- Input-output techniques should be developed for a more robust and fully automatic modal identification;
- The sampler should to be tested on different materials and in-situ conditions.

The new variant needs more refining to develop to real context use. Some of the possible works/developments are:

- Develop a custom made ‘calibrated’ bar in which each of the parameters is careful controlled/determined;
- Study the model with other mixtures or materials;
- The embedment length and beginning of the cantilevered region should be verified carefully (e.g. though a microscope);
- Reduce the uncertainty of some relevant parameters for E-modulus estimation.



## 7 Bibliography

- Adam, C. & Adam, D., 2003. Modelling of the dynamic load plate test with the light falling weight device. *Asian Journal of Civil Engineering*, 4, pp.73–89.
- Alvarado, G. & Coop, M., 2012. On the Performance of Bender Elements in Triaxial Tests. *Geotechnique*, 62.
- Amu, O.O., Bamisaye, O.F. & Komolafe, A.I., 2011. The Suitability and Lime Stabilization Requirement of Some Lateritic Soil Samples as Pavement. *International Journal of Pure and Applied Sciences and Technology*, pp.29–46.
- Anifowose, A.Y.B., 1989. The performance of some soils under stabilization in Ondo State, Nigeria. *Bulletin of the International Association of Engineering Geology - Bulletin de l'Association Internationale de Géologie de l'Ingénieur*, 40(1), pp.79–83.
- Azenha, M., 2009. *Numerical simulation of the structural behaviour of concrete since its early ages*. Universidade do Porto.
- Azenha, M., Barros, J., Granja, J. & Sousa, C., 2012. *Aproveitamento Hidroelétrico de Salamonde – Reforço de potência: Apoio à caracterização do endurecimento do betão no âmbito da utilização de cofragens deslizantes*,
- Baligh, M.M., Azzouz, A.S. & Chin, C.T., 1987. Disturbances due to “ideal” tube sampling.
- Bell, F.G., 2004. *Engineering Geology and Construction*, CRC Press.
- Bell, F.G., 1993. *Engineering Treatment of Soils: Soil Stabilization*, London.
- Benz, T., 2007. *Small-strain stiffness of soils and its numerical consequences*. Universitat Stuttgart.
- Briaud, J.-L., 2013. *Geotechnical Engineering: Unsaturated and Saturated Soils*, John Wiley & Sons, Inc.
- Brignoli, E., Gotti, M. & Stokoe, K., 1996. Measurement of shear waves in laboratory specimens by means of piezoelectric transducers. *ASTM geotechnical testing journal*, 2.
- Clayton, C., Siddique, A. & Hopper, R.J., 1998. Effects of sampler design on tube sampling disturbance-numerical and analytical investigations.
- Clayton, C.R. ;, Matthews, M.C. & Simons, N.E., 1995. Site Investigation.
- Consoli, N.C., Rosa, D.A., Cruz, R.C. & Rosa, A.D., 2011. Water content, porosity and cement content as parameters controlling strength of artificially cemented silty soil. *Engineering Geology*, 122(3-4), pp.328–333.

- Costa, S., 2011. *Tecnologias Avançadas para a Determinação do Módulo de Deformabilidade de Solo-Cimento desde as Primeiras Idades*. Universidade do Minho.
- Datasheet Cimpor, 2004. *GUIÃO TÉCNICO- CIMENTO PORTLAND DE CALCÁRIO CEM II / B-L 32.5N CEM II/A-L 42.5R*,
- Fang, H.-Y., 1990. *Foundation Engineering Handbook*,
- Ferreira, C., 2009. The use of seismic wave velocities in the measurement of stiffness of a residual soil.
- Gomes Correia, A., 2004. Soil stiffness interesting the serviceability of structures. *Geotecnica*, 100, pp.103–122.
- Gomes Correia, A., Antão, A. & Gambin, M., 2004. Using a non linear constitutive law to compare Menard PMT and PLT E-moduli. In *Proceedings ISC-2 on Geotechnical and Geophysical Site Characterization*. Rotterdam: Millpress.
- Gomes Correia, A., MARTINS, J., CALDEIRA, L., MARANHA DAS NEVES, E. & DELGADO, J., 2009. Comparison of in situ performance-based tests methods to evaluate moduli of railway embankments. *AL-QADI, T. (ed.) Bearing Capacity of Roads, Railways and Airfields*.
- Gomes Correia, A., Reis Ferreira, S.M. & Faria Araújo, N., 2006. Precision triaxial tests to determine deformability characteristics. In *Proceedings of the 10th national congress on geotechnics*. Lisbon, pp. 317–326.
- Gomes Correia, A., Viana da Fonseca, A. & Gambin, M., 2004. Routine and advanced analysis of mechanical in situ tests. Results on saprolitic soils from granites more or less mixed in Portugal. In *Proceedings ISC-2 on Geotechnical and Geophysical Site Characterization*. Rotterdam: Millpress.
- Hmtri, 1997. *Site Characterization: Sampling and Analysis 1997* John Wiley & Sons, ed.,
- Horpibulsuk, S., Katkan, W., Sirilerdwattana, W. & Rachan, R., 2006. Strength development in cement stabilized low plasticity and coarse grained soils: Laboratory and field study. *Soils and Foundations*, 46(3), pp.351–366.
- Houlsby, G.T., Amorosi, A. & Rojas, E., 2005. Elastic moduli of soils dependent on pressure: a hyperelastic formulation. *Geotechnique*, 55(5), pp.383–392.
- Hunt, R.E., 2005. *Geotechnical Engineering Investigation Handbook Second Edi.*,
- Hvorslev, M.J., 1949. *Subsurface exploration and sampling of soils for civil engineering purposes*, Vicksburg.
- Johnson, H.L., 1940. Improved sampler and sampling technique for cohesionless soils. *Civil Engineering*, 10.
- Kelleher, P., Geotech, B. & Hull, T., 2008. Quality Assesment of Marine Sediments Recovered with a Hydraulically Tethered Piston Corer.

- Kennedy, T.W., Smith, R. & Holmgreen Jr, R.J. Tahmoressi, M., 1987. An evaluation of lime and cement stabilization. *Transportation Research Record*, 119, pp.11–25.
- Landon, M.M., 2007. *Development of a Non-destructive Sample Quality Assessment Method for Soft Clays*. University of Massachusetts.
- Lefebvre, G. & Poulin, C., 1979. A new method of sampling in sensitive clay.
- Magalhães, F., 2012. *Identificação modal estocástica para validação experimental de modelos numéricos*. Universidade do Porto.
- Magalhães, N., 2013. *Influência dos parâmetros da formulação na rigidez de solos estabilizados: estudo experimental*. Universidade do Minho.
- Marcuson III, W.F. & Franklin, A.G., 1979. STATE OF THE ART OF UNDISTURBED SAMPLING OF COHESIONLESS SOILS.
- Marjanovic, J., 2012. *The study of shear and longitudinal velocity measurements of sands and cohesive soils*. Massachusetts Institute of Technology.
- Meredith, N., 1999. Determination of the elastic modulus of resin based materials as a function of resonance frequency during polymerisation. *Dental Materials*, 15, pp.98–104.
- Meyers, M.A. & Chawla, K.K., 2008. *Mechanical Behavior of Materials* Cambridge., New York.
- Murthy, V.N.S., 2002. *Geotechnical Engineering: Principles and Practices of Soil Mechanics and Foundation Engineering*, CRC Press.
- Nagaraj, H.B., Sravan, M.V., Arun, T.G. & Jagadish, K.S., 2014. Role of lime with cement in long-term strength of Compressed Stabilized Earth Blocks. *International Journal of Sustainable Built Environment*, 3(1), pp.54–61. Available at: <http://www.sciencedirect.com/science/article/pii/S2212609014000120> [Accessed November 2, 2014].
- Nagaraj, T.J., 1993. *Principles of Testing Soils, Rocks and Concrete*,
- National Cooperative Highway Research Program, 2009. *NDT Technology for Quality Assurance of HMA Pavement Construction*,
- Osterberg, J.O., 1973. An improved hydraulic piston sampler.
- Portelinha, F.H.M., Lima, D.C., Fontes, M.P.F. & Carvalho, C.A.B., 2012. Modification of a Lateritic Soil with Lime and Cement: An Economical Alternative for Flexible Pavement Layers.
- Quigley, P., 2006. Modification / Stabilisation of Low Strength Cohesive Soils under Foundations and Floor Slabs.
- Raymond, G.P., 1977. Effect on soil sampling on the drained properties of Leda Clay’.
- Rogers, J.D., 2006. Subsurface Exploration Using the Standard Penetration Test and the Cone Penetrometer Test. *Environmental & Engineering Geoscience*, XII, pp.161–179.

- Siddique, A., Ameen, S.F. & Islam, M.J., 2006. A comparative study on engineering properties of “Block” and “Tube” samples of a soft clay.
- Siddique, A.B.U., 1990. A NUMERICAL AND EXPERIMENTAL STUDY OF SAMPLING DISTURBANCE.
- Silva, J., 2010. *Contribuição para o estudo do tratamento de solos: Avaliação da deformabilidade*. Universidade do Minho.
- Silva, J., Azenha, M., Gomes Correia, A. & Ferreira, C., 2013. Continuous stiffness assessment of cement-stabilised soils from early age. *Geotechnique*.
- Silva, J., Azenha, M., Gomes Correia, A. & Granja, J., 2014. Continuous monitoring of sand–cement stiffness starting from layer compaction with a resonant frequency-based method: Issues on mould geometry and sampling. *Soils and Foundations* 54.
- Stephenson, R.W., 1978. Ultrasonic testing for determining dynamic soil moduli. *ASTM STP 654, American Society for Testing and Materials*.
- Tanaka, H., 2008. Sampling and sample quality of soft clays.
- Terzaghi, K. & Peck, R., 1948. *Soil Mechanics in Engineering Practice* J. Wiley, ed., New York.
- UNI EN, 2007. BS EN 1997-2:2007 - Eurocode 7: Geotechnical design - Part 2: Ground investigation and testing. In *Eurocode 7*.
- Viana da Fonseca, A., Cruz, R.C. & Consoli, N.C., 2009. Strength Properties of Sandy Soil–Cement Admixtures. *Geotechnical and Geological Engineering*, 27, pp.681–686.
- Voigt, T., Sun, Z. & Shah, S.P., 2006. Comparison of ultrasonic wave reflection method and maturity method in evaluating early-age compressive strength of mortar. *ement and Concrete Composites*, 28.
- Welch, P., 1967. The use of fast Fourier transform for the estimation of power spectra: A method based on time averaging over short modified periodograms. *IEEE Transaction on Audio and Electro-Acoustics*, 15(2), pp.70–73.
- Yesiller, N., Hanson, J.L. & Usmen, M., 2001. Ultrasonic Assessment of Stabilized Soils.